



NRC Publications Archive Archives des publications du CNRC

Determination of indoor humidity profile using a whole-building hygrothermal model

Tariku, F.; Kumaran, M. K.; Fazio, P.

This publication could be one of several versions: author's original, accepted manuscript or the publisher's version. /
La version de cette publication peut être l'une des suivantes : la version prépublication de l'auteur, la version
acceptée du manuscrit ou la version de l'éditeur.

For the publisher's version, please access the DOI link below. / Pour consulter la version de l'éditeur, utilisez le lien
DOI ci-dessous.

Publisher's version / Version de l'éditeur:

<http://dx.doi.org/10.1007/s12273-011-0031-x>

Building Simulation, 4, 1, pp. 61-78, 2011-03-01

NRC Publications Record / Notice d'Archives des publications de CNRC:

<http://nparc.cisti-icist.nrc-cnrc.gc.ca/npsi/ctrl?lang=en>

<http://nparc.cisti-icist.nrc-cnrc.gc.ca/npsi/ctrl?lang=fr>

Access and use of this website and the material on it are subject to the Terms and Conditions set forth at

http://nparc.cisti-icist.nrc-cnrc.gc.ca/npsi/jsp/nparc_cp.jsp?lang=en

READ THESE TERMS AND CONDITIONS CAREFULLY BEFORE USING THIS WEBSITE.

L'accès à ce site Web et l'utilisation de son contenu sont assujettis aux conditions présentées dans le site

http://nparc.cisti-icist.nrc-cnrc.gc.ca/npsi/jsp/nparc_cp.jsp?lang=fr

LISEZ CES CONDITIONS ATTENTIVEMENT AVANT D'UTILISER CE SITE WEB.

Contact us / Contactez nous: nparc.cisti@nrc-cnrc.gc.ca.





Determination of indoor humidity profile using a whole-building hygrothermal model

NRCC-53993

Tariku, F.; Kumaran, M.K.; Fazio, P.

April 2011

A version of this document is published in / Une version de ce document se trouve dans:
Building Simulation, 4, (1), pp. 61-78, March 01, 2011, DOI: [10.1007/s12273-011-0031-x](https://doi.org/10.1007/s12273-011-0031-x)

The material in this document is covered by the provisions of the Copyright Act, by Canadian laws, policies, regulations and international agreements. Such provisions serve to identify the information source and, in specific instances, to prohibit reproduction of materials without written permission. For more information visit <http://laws.justice.gc.ca/en/showtdm/cs/C-42>

Les renseignements dans ce document sont protégés par la Loi sur le droit d'auteur, par les lois, les politiques et les règlements du Canada et des accords internationaux. Ces dispositions permettent d'identifier la source de l'information et, dans certains cas, d'interdire la copie de documents sans permission écrite. Pour obtenir de plus amples renseignements : <http://lois.justice.gc.ca/fr/showtdm/cs/C-42>



National Research
Council Canada

Conseil national
de recherches Canada

Canada

DETERMINATION OF INDOOR HUMIDITY PROFILE USING A WHOLE-BUILDING HYGROTHERMAL MODEL

Fitsum Tariku^{1*}, Kumar Kumaran², Paul Fazio³

¹British Columbia Institute of Technology, 3700 Willingdon Ave., Burnaby,

British Columbia, Canada V5G 3H2

²National Research Council, Institute for Research in Construction, 1200 Montreal rd.,

Ottawa, Ontario, Canada, K1A 0R6

³Concordia University, Building, Civil and Environmental Engineering Department,

1455 de Maisonneuve Blvd. West, Montreal, Quebec, Canada, H3G 1M8

* Corresponding author: 3700 Willingdon Ave., BCIT, Burnaby, Canada V5G 3H2;

Fitsum_Tariku@bcit.ca

Abstract

During the design of a new building or retrofitting of an existing one, it is important to reliably assess the indoor humidity levels of the building as it can potentially affect the building envelope durability, occupants' comfort and health risks associated with mould growth. Simplistic assumptions of indoor humidity profiles, which ignore the dynamic coupling of the indoor environment and building enclosure, may lead to inaccurate conclusions about the indoor environment and moisture performance of the building enclosure. In this paper, a whole-building hygrothermal model called HAMFitPlus, which takes into account the dynamic interactions between building envelope components, mechanical systems and indoor heat and moisture generation mechanisms, is used to assess the indoor humidity condition of an existing occupied house. HAMFitPlus is developed on SimuLink development platform and integrates COMSOL multiphysics with MatLab. The basic input parameters of the model are discussed in detail, and its simulation results are presented. In general, the HAMFitPlus simulation results are in good agreement with the measured data.

Keywords: coupled HAM analysis, whole-building hygrothermal modeling, energy efficiency, indoor environment, building envelope performance

NOMENCLATURE

A_c condensate surface area (m^2)	h_{fg} latent heat of evaporation/condensation (J/kg)
A_i surface area of surface i (m^2)	h_o outdoor surface heat transfer coefficient ($W/(K \cdot m^2)$)
A_e evaporative surface area (m^2)	I_o incident solar radiation (W/m^2)
A_w window surface area (m^2)	k_a air flow coefficient (s)
Cv_m specific capacity of solid matrix (J/(K·kg))	\dot{m} mass flow rate of dry air (kg/s)
Cp_a specific capacity of air (J/(K·kg))	\dot{m}_c moisture condensation/evaporation rate (kg/s)
Cp_v specific capacity of water vapor (J/(K·kg))	\dot{m}_m mass flow rate of dry air (humidification/dehumidification systems) (kg/s)
Cp_l specific capacity of liquid water (J/(K·kg))	\dot{m}_h mass flow rate of dry air (heating/cooling systems) (kg/s)
D_l liquid conductivity (s)	M molecular mass of water molecule (0.01806 kg/mol)
f_{sa} solar air factor (-)	p zone vapour pressure (Pa)
\bar{g} acceleration due to gravity (m/s^2)	P_{atm} atmospheric pressure (Pa)
h_i^m mass transfer coefficient of surface i ($kg/(Pa \cdot s \cdot m^2)$)	P total pressure (Pa)
h_i^h heat transfer coefficient of surface i ($W/(K \cdot m^2)$)	P_v vapour pressure (Pa)
h_c^m mass transfer coefficient for condensate surface ($kg/(Pa \cdot s \cdot m^2)$)	\hat{P} saturated vapor pressure (Pa)
h_e^m mass transfer coefficient for evaporation surface ($kg/(Pa \cdot s \cdot m^2)$)	p_i^s surface vapor pressure of surface i (Pa)
	\hat{p}_e saturated vapor pressure of reservoir e (Pa)

\hat{p}_c saturated vapor pressure of condensate c (Pa)	τ solar transmittance (-)
\dot{Q}_s heat source (W/m ³)	ω humidity ratio (kg/kg dry air)
R universal gas constant (8.314 J/mol)	ω_e humidity ratio of outdoor air (kg/kg dry air)
T temperature (°C)	$\tilde{\omega}$ set point humidity ratio (kg/kg dry air)
T_e outdoor air temperature (°C)	δ_v vapor permeability (s).
T_i^s surface temperature of surface i (°C)	Θ sorption capacity (kg/m ³)
\tilde{T} set point temperature (°C)	
U overall heat transfer coefficient (W/(K·m ²))	
\vec{u} air velocity (m/s)	
\tilde{V} volume of the zone (m ³)	
Y_l mass fraction of liquid water (-)	
<u><i>Greek letters</i></u>	
α solar absorptance (-)	
ϕ relative humidity (-)	
ρ_a density of air (kg/m ³)	
ρ_w density of water (kg/m ³)	
ρ_m density of material (kg/m ³)	
λ_{eff} effective thermal conductivity (W/(m.K))	
η dynamic viscosity (kg/(m.s))	

1. INTRODUCTION

Accurate prediction of indoor conditions, more specifically indoor temperature and relative humidity, are important for the following four reasons: 1) To better assess the hygrothermal performance of building envelope components (Tsongas et al., 1996; Tariku et al., 2009) and reduce the likelihood of building envelope failure. High indoor humidity can result in excess moisture accumulation in the structures and deterioration of components due to mold/decay or corrosion. 2) To maintain the critical relative humidity range, which is specific to the building's operation (Trechsel, 2001; Rode, 2003). For example, churches, museums and libraries need to maintain an optimum relative humidity to avoid moisture damage on paintings, artifacts and books. 3) To create an acceptable indoor air quality. Unless controlled, high relative humidity, which is a favorable condition for mold growth, can cause health problems for occupants and damage to the interior lining of the building (Sterling et al., 1985; Clausen et al., 1999; Oreszczyn and Pretlove, 1999). 4) To create a comfortable environment for occupants as recommended in ASHRAE Standard 55-1992 and ASHRAE Standard 62-1999. The satisfaction and dissatisfaction of occupants are related to the level of indoor relative humidity and temperature (Toftum et al., 1998; Fang et al., 1998a,b).

Various models have been developed in the past to predict the humidity level of the indoor environment. These models can be broadly categorized into three groups: 1) The first group consists of empirical models, which are based on large-scale field measurement data of various buildings. In these models the indoor vapor pressure is estimated from the outdoor temperature (Sandberg, 1995) or outdoor vapor pressure (Abranties and Freitas, 1989). The factors that determine the actual indoor humidity level such as internal moisture source, ventilation/air leakage, absorption/desorption effect of building material, and other factors are masked and

represented by a single parameter called occupant type. These models at best can be good for a rough estimation of the indoor humidity especially for summer conditions when the natural ventilation could be higher. 2) The second group of models is based on steady state analysis of moisture balance. These models are more detailed, and need specific information about the building such as building volume, air-exchange-rate (ACH) and occupant behavior in relation to moisture production/removal. In this category of models the only moisture transport mechanism is by ventilation (Loudon, 1971; Hutcheon and Handegord, 1995; Tsongas et al., 1996; TenWolde, 2001). Ventilation rate and moisture generation need to be explicitly defined, but the moisture absorption and release by the interior furnishing and furniture are differed in these models as well. 3) The third group of models is an improvement on the second group, and based on an isothermal transient analysis of humidity balance differential equation. In these models the moisture buffering effects of internal furnishing are accounted for in simplified ways. In humidity prediction models, the moisture buffering effects are represented in many ways with various simplifying assumptions. In the early 1980s Tsuchiya presented an indoor relative humidity model where the moisture buffering effect of interior surfaces is given by an empirical expression. As it is presented in Kusuda's (1983) paper, the moisture exchange between the indoor air and the moisture buffering material is limited to the contact surface only.

TenWolde (1988) developed a mathematical model called FPLRH1 where the moisture storage effect of hygroscopic materials is empirically calculated. Later, TenWolde (1994) upgraded his indoor humidity model FPLRH1 to FPLRH2. In this improved model, the moisture buffering effect of the interior furnishing materials is related to the exponentially weighted back average of indoor relative humidity, which gives more weight for recent humidity conditions, rather than the arithmetic average as used in the earlier model. The other variant of this class of indoor model is

the Jones model (1993, 1995), which considers the indoor moisture generation and ventilation rate as well as the absorption/desorption effect. The absorption/desorption characteristics of the interior furnishing are represented by two empirical coefficients called moisture admittance factors, one representing moisture absorption and the other representing desorption. As Kumaran (2005) pointed out, the models in this category and identified by Jones (1995) as “current humidity models” are similar to the early work of Tsuchiya, and only vary in the assumption made in representing the terms, particularly the moisture absorption/desorption by moisture buffering materials. Because of their underlying assumption of constant moisture content, these models may not capture the dynamic responses of the moisture buffering material to a transient or abrupt moisture production/removal in the indoor air. To capture this dynamic process, El Diasty et al. (1992, 1993) developed an advanced humidity model using a transient heat transfer analysis analogy. In their work, the moisture buffering response of materials is modeled assuming the moisture exchange between the material and the indoor air is limited to a few millimeters depth of the material, or with no moisture gradient across the material (lumped system) for cases where the surface resistance is large compared to the internal resistance for moisture flow. The challenges in this modeling approach are in defining the critical penetration depth, which could be arbitrary, and also the applicability of a lumped-capacity assumption in real conditions.

In reality the indoor conditions are determined by performing an integrated analysis of the heat and mass balance of the external and internal loading as well as the mechanical systems’ outputs.

In the recently concluded IEA¹/Annex 41 international research project “Whole building heat, air, moisture response—MOIST-ENG” this holistic approach was applied to a single zone

¹ International Energy Agency

building (Woloszyn and Rode, 2008). The experimental and numerical test cases that were generated during the project are used for benchmarked the whole-building hygrothermal model (HAMFitPlus) used in this paper (Tariku et al., 2010b).

Unlike the models discussed earlier, where the indoor humidity is predicted with a simplified or no coupling with the building envelope components, HAMFitPlus, a transient and non-isothermal model, takes into account the dynamic interaction between indoor environment and building enclosure. In addition the model incorporates among other things the following: moisture buffering effects of materials which could act as a moisture source and sink; moisture removal due to condensation on cold surfaces such as on windows; moisture addition by evaporation from water reservoirs and from building envelope components that have higher initial moisture content, as well as moisture flow through building envelope components (walls, roof, foundation walls and floor slabs) by diffusion and convection. The model integrates building envelope enclosures, indoor environment, HVAC systems, and indoor heat and moisture generation mechanisms, and simultaneously predicts the indoor temperature and humidity conditions, building envelope moisture conditions and energy consumption of a building in response to time-varying weather conditions. In this paper, HAMFitPlus is used to assess the indoor humidity condition of a residential house. Following a brief description of the model, the model's input parameters are discussed, and the simulation results are compared with measured results.

2. BRIEF DESCRIPTION OF THE WHOLE BUILDING HYGROTHERMAL MODEL - HAMFitPlus

In HAMFitPlus simulation, the building is considered as an integrated system, which consists of building enclosure, indoor environment, and mechanical systems. Thus the indoor conditions, more specifically, temperature and relative humidity, are unknown quantities, and have to be determined from the heat and mass balance at the zone considering the three processes: 1) heat and mass transfer across building enclosure 2) internal heat and moisture generation by occupants and their activities, and 3) heat and moisture supply by mechanical systems (heating, cooling, humidification, dehumidification and ventilation) depending on the mode of operation of the building. To deal with these inter related and coupled processes, an integrated and coupled modeling approach, which integrates the dynamic HAM transfer of the building envelope with the indoor environment and its components (HVAC system, moisture and heat sources) is necessary. Here, building envelope and indoor models are developed independently and coupled to form the whole building hygrothermal model, HAMFitPlus. The mathematical descriptions of these primary models are presented below.

2.1. Building envelope model

The building envelope model solves, simultaneously, the three interdependent transport phenomena of heat, air and moisture (HAM) in a building component. The mathematical model is based on building physics and comprises a set of partial differential equations (PDEs) that govern the individual flows. The corresponding governing equations are as follows:

Moisture balance:

$$\Theta \frac{\partial \phi}{\partial t} = \nabla \cdot (D_\phi \nabla \phi + D_T \nabla T) - \nabla \cdot (D_l \rho_w \bar{g} + \rho_a \bar{u} C_c \bar{P} \phi) \quad (1)$$

where $D_\phi = \left(\delta_v \bar{P} + D_l \frac{\rho_w R T}{M \phi} \right)$, $D_T = \left(\delta_v \phi \frac{\partial \bar{P}}{\partial T} + D_l \frac{\rho_w R}{M} \ln(\phi) \right)$ and $C_c = \frac{0.622}{P_{atm}}$

Heat balance:

$$\begin{aligned} \rho_m C_{p_{eff}} \frac{\partial T}{\partial t} + \nabla \cdot (\bar{u} T) \rho_a (C_{p_a} + \omega C_{p_v}) + \\ \nabla \cdot (-\lambda_{eff} \nabla T) = \dot{m}_c h_{fg} + \dot{m}_c T (C_{p_v} - C_{p_l}) + \dot{Q}_s \end{aligned} \quad (2)$$

where $C_{p_{eff}} = C_{v_m} + Y_l C_{p_l}$ and $\dot{m}_c = \nabla \cdot (\delta_v \nabla P_v) - \rho_a \nabla \cdot (\bar{u} \omega)$

Air mass balance:

$$\nabla \cdot (\rho_a \bar{u}) = 0 \quad (3)$$

Momentum balance (Darcy equation)

$$\bar{u} = -\frac{k_a}{\eta} \nabla P \quad (4)$$

$$-\nabla \cdot \left(\rho_a \frac{k_a}{\eta} \nabla P \right) = 0 \quad (5)$$

In the moisture balance equation, Equation (1), relative humidity is the driving potential. The l.h.s term represents the rate of change of moisture accumulation; and the moisture transport due to relative humidity and temperature gradients are represented by the first and second terms of the r.h.s of Equation (1), respectively. The third and fourth l.h.s terms represent liquid water transport by gravity and water vapor transport by convection, respectively. Temperature is the driving potential for the heat balance equation, Equation (2). The transfer of heat by convection and diffusion are represented by second (l.h.s) and first (r.h.s) terms of the equations, respectively. The latent and sensible heat sources or sinks associated with phase changes are represented by the first and second terms of the right hand side of the equation. Any other internal heat source or sink is given by the last term of the of the right hand side of the equation. The mass balance equation for incompressible fluid is given by Equation (3). In a building physics application, the air is considered as incompressible due to very low airflow speeds, and low pressure and temperature changes. The Darcy equation, Equation (4), is a reduced form of the Navier-Stokes momentum equation for flow in a porous media. Combing the mass balance, (Equation(3)) and momentum balance (Equation (4)) equations gives Equation (5).

The governing PDEs of the three transport phenomena (Equation(1), Equation (2) and Equation (5)) are coupled and solved simultaneously for temperature, relative humidity and pressure using

a finite element based software called COMSOL Multiphysics². This commercial software is found to be beneficial for solving non-standard coupled-multiphysics problems because of its open provision for implementing user-defined PDEs. The model accommodates non-linear transfer and storage properties of materials, moisture transfer by vapor diffusion, capillary liquid water transport, and convective heat and moisture transfer through multi-layered porous media. The transient HAM model is successfully benchmarked against published test cases (Tariku, 2008; Tariku et al., 2010a). The test cases are comprised of an analytical verification, comparisons with other models, and validation of simulation results with experimental data.

2.2. Indoor model

The indoor model is developed to predict the indoor temperature and humidity conditions based on the heat and moisture balance in a zone, by accounting for all the heat and moisture fluxes which cross the zone boundaries, and also for the internal heat and moisture generation/removal from the zone due to the operating condition of the building or occupant behavior. The basic assumption of the model is that the indoor air is well mixed and can be represented by a single node. Under this assumption, the following two linear first-order differential equations for moisture and heat balances are developed:

Indoor humidity balance:

The humidity balance equation developed in this work incorporates the moisture absorption/desorption of hygroscopic internal lining of building envelope components and furniture (\dot{Q}_b^m); moisture supply and removal from the zone by airflow (\dot{Q}_v^m), moisture addition

² <http://www.comsol.com>

and removal by mechanical systems (\dot{Q}_m^m), moisture addition into zone due to occupant activities (\dot{Q}_o^m), evaporation from sink or bath tub (\dot{Q}_e^m), and moisture removal due to moisture condensation on surfaces (\dot{Q}_c^m). The indoor humidity model is mathematically represented by Equation (6) below:

$$\rho_a \tilde{V} \frac{d\omega}{dt} = \dot{Q}_b^m + \dot{Q}_v^m + \dot{Q}_m^m + \dot{Q}_e^m + \dot{Q}_c^m + \dot{Q}_o^m \quad (6)$$

where:

$$\begin{aligned} \dot{Q}_b^m &= \sum_i A_i h_i^m (p_i^s - p); & \dot{Q}_v^m &= \dot{m}(\omega_e - \omega); \\ \dot{Q}_m^m &= \dot{m}_m (\tilde{\omega} - \omega) \leq \dot{Q}_{m_max}^m; & \dot{Q}_e^m &= \sum_e A_e h_e^m (\hat{p}_e - p) \\ \dot{Q}_c^m &= \sum_c A_c h_c^m (\hat{p}_c - p) \end{aligned}$$

The term $\dot{Q}_{m_max}^m$ is the maximum moisture supply or removal capacity of the humidification or dehumidification systems, respectively.

Indoor energy balance:

The general energy balance equation for the indoor air considers the energy exchange between the building envelope internal surfaces and the indoor air (\dot{Q}_b^h), the energy carried by the air flow into and out of the zone (\dot{Q}_v^h), the heat supply and removal (heating/cooling) by mechanical systems to maintain the room in the desired temperature range (\dot{Q}_m^h), the internal

heat generated due to occupant activities (e.g. cooking) and building operation (e.g. lighting) (\dot{Q}_o^h), the energy supplied and removed from the interior space due to enthalpy transfer by moisture movement (\dot{Q}_m^h), and heat gain through the fenestration system (\dot{Q}_f^h). The contribution of each term in the total energy balance equation is described below. For the purpose of energy balance, the indoor air is assumed to be a mixture of dry air and water vapor only. Hence, the indoor energy balance in terms of mixture enthalpy is given by Equation (7).

$$\rho_a \tilde{V} \frac{dh}{dt} = \dot{Q}_b^h + \dot{Q}_v^h + \dot{Q}_m^h + \dot{Q}_f^h + \dot{Q}_h^h + \dot{Q}_o^h \quad (7)$$

$$\text{where: } \dot{Q}_b^h = \sum_i A_i h_i^h (T_i^s - T); \quad \dot{Q}_v^h = \dot{m} C p_a (T_e - T);$$

$$\dot{Q}_m^h = \dot{m}_h (C p_a + \omega C p_v) (\tilde{T} - T) \leq \dot{Q}_{m_max}^h;$$

$$\dot{Q}_f^h = A_w \cdot \left(\underbrace{\frac{U (T_e - T)}{\text{due to temperature difference}}}_{\text{fraction of absorbed solar radiation}} + \underbrace{\frac{U}{h_o} \alpha I_o}_{\text{fraction of transmitted solar radiation}} + \underbrace{f_{sa} \tau I_o}_{\text{fraction of transmitted solar radiation}} \right)$$

$\dot{Q}_{m_max}^h$ is the maximum sensible heating and cooling available from the respective equipment.

The term \dot{Q}_h^h accounts for the sensible and latent heat transfer that are generated due to moisture movement by ventilation (\dot{Q}_v^m) and convection at the building envelope surfaces (\dot{Q}_b^m); moisture gain or removal from the indoor space by mechanical systems (humidification/dehumidification) (\dot{Q}_m^m), and also other means: occupant activity (\dot{Q}_o^m), evaporation (\dot{Q}_e^m) and condensation (\dot{Q}_c^m).

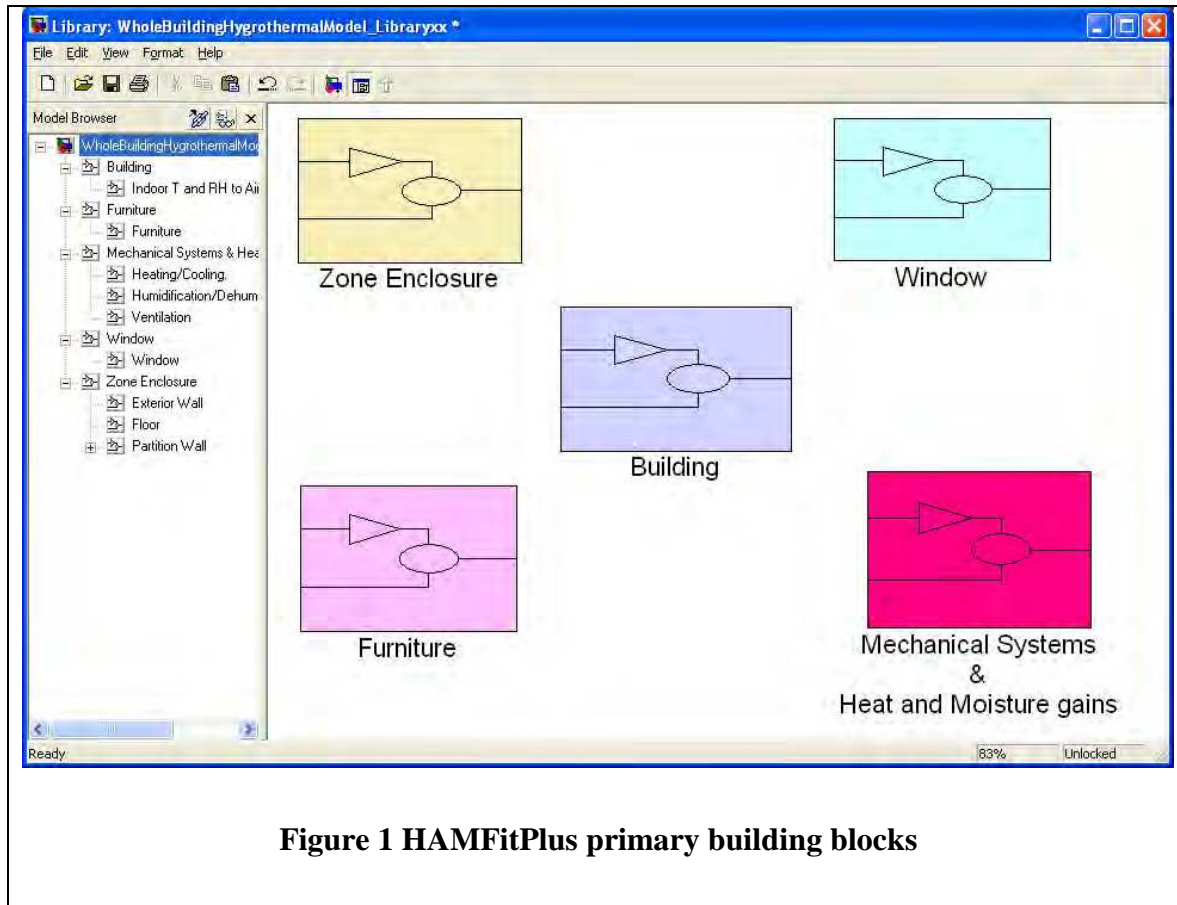
The moisture and heat additions into the zone due to occupant activities (\dot{Q}_o^m and \dot{Q}_o^h) are usually independent of the indoor condition; rather, they depend on occupant behavior. To reflect occupant activities at various times, diurnal moisture and heat generation rate schedules are used in the indoor humidity and energy calculations. These coupled and non-linear indoor humidity and energy balance equations, Equations (6) and (7), respectively, are simultaneously solved for indoor humidity and temperature using SimuLink and MatLab.

2.3. Whole building hygrothermal model (HAMFitPlus)

The whole building hygrothermal model, HAMFitPlus, is developed on SimuLink simulation environment, which provides a smooth interface with the COMSOL Multiphysics and MatLab³ computational tools. The simulation environment allows full integration and dynamic coupling of the building envelope model (Section 2.1) and indoor model (Section 2.2) using the special SimuLink block called S-Function. As shown in Figure 1, the HAMFitPlus model comprises five primary blocks: “Building”, “Zone Enclosure”, “Window”, “Furniture” and “Mechanical Systems and Heat and Moisture gains”. In each block, a “user-developed” S-function algorithm, which describes the task, inputs and outputs of each block, is written in MatLab programming language and embedded. This approach permits full control of the simulation environment and is particularly useful in the whole building hygrothermal analysis where there is large time scale variation between building enclosure and HVAC systems response (Schijndel and Hensen, 2005). The HAMFitPlus model can be classified as a hybrid model, with a continuous part for the indoor model and a discrete part for the building envelope model. The simulation update time

³ <http://www.mathworks.com>

for the discrete part is user-specified, and can vary from seconds to hours depending on the boundary conditions. The blocks have graphical user interfaces (GUIs) to enter user-specified data.



The general specification of the building, including the building site (latitude, longitude, altitude, topography and surrounding environment), the building size and orientation, and the surface area, orientation, inclination and air tightness of the building envelope components, are specified in the “Building” block. The zone humidity and energy balance equations are encapsulated in this block. The integration of different blocks creates a virtual simulation environment as presented in Figure 2. The “Zone enclosure” block encapsulates the six building envelope components (roof, floor and four walls). The building envelope components can be

composed of different layers of materials and thickness, and can also be exposed to different exterior boundary conditions. For example, in Figure 3, the south and east walls are exterior walls, the north and west walls are partition walls that are adjacent to the hallway and next room, respectively, and the other two components are the ceiling and floor. The inputs to each component block are the indoor temperature and relative humidity, and the outputs of the blocks are the interior surface temperature and humidity conditions of the components based on one-dimensional HAM analysis. Each building envelope component has a GUI, as shown in Figure 4, to specify the number and type of material layers, thickness, initial conditions, surface heat and moisture transfer conditions and mesh sizes at the boundaries and domain of each material.

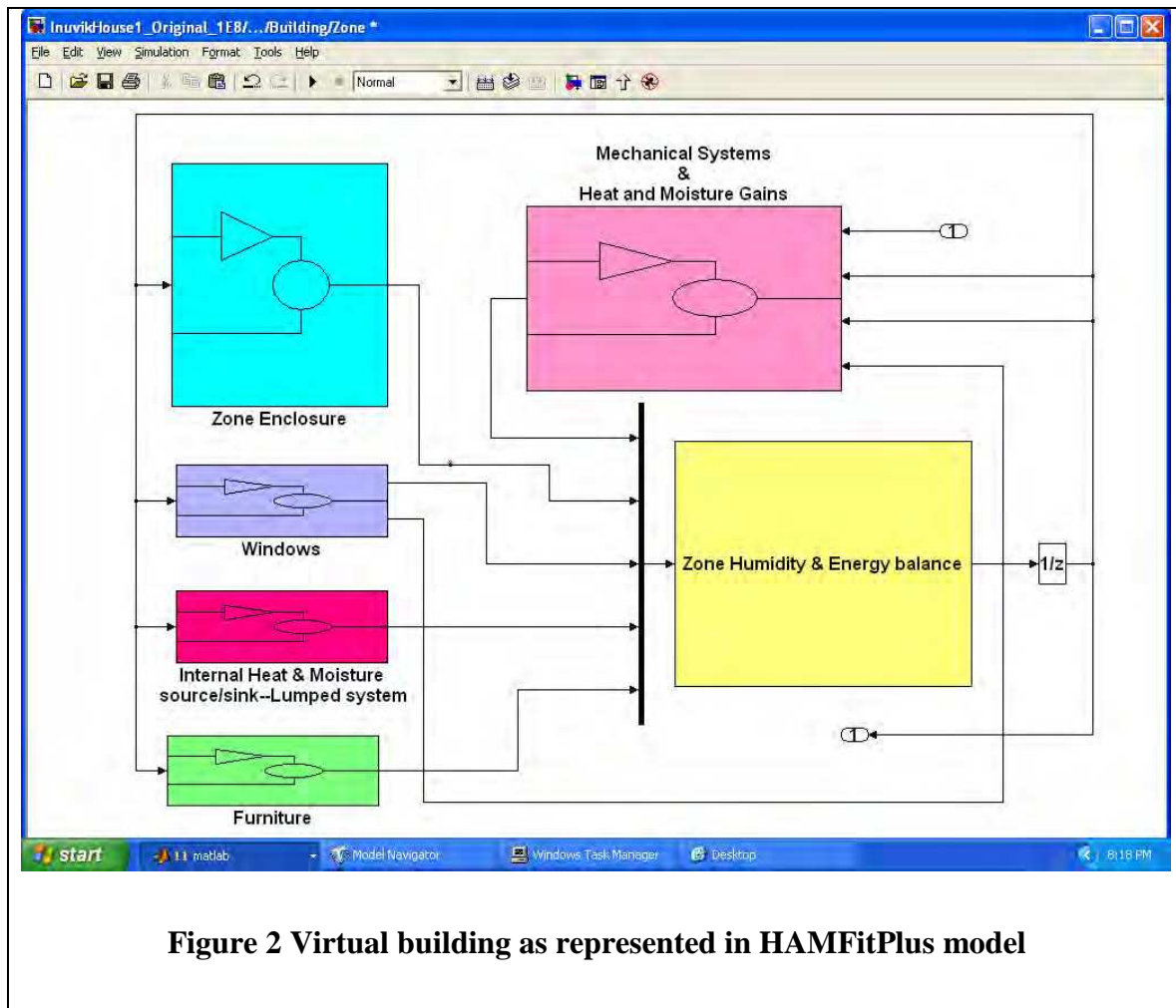


Figure 2 Virtual building as represented in HAMFitPlus model

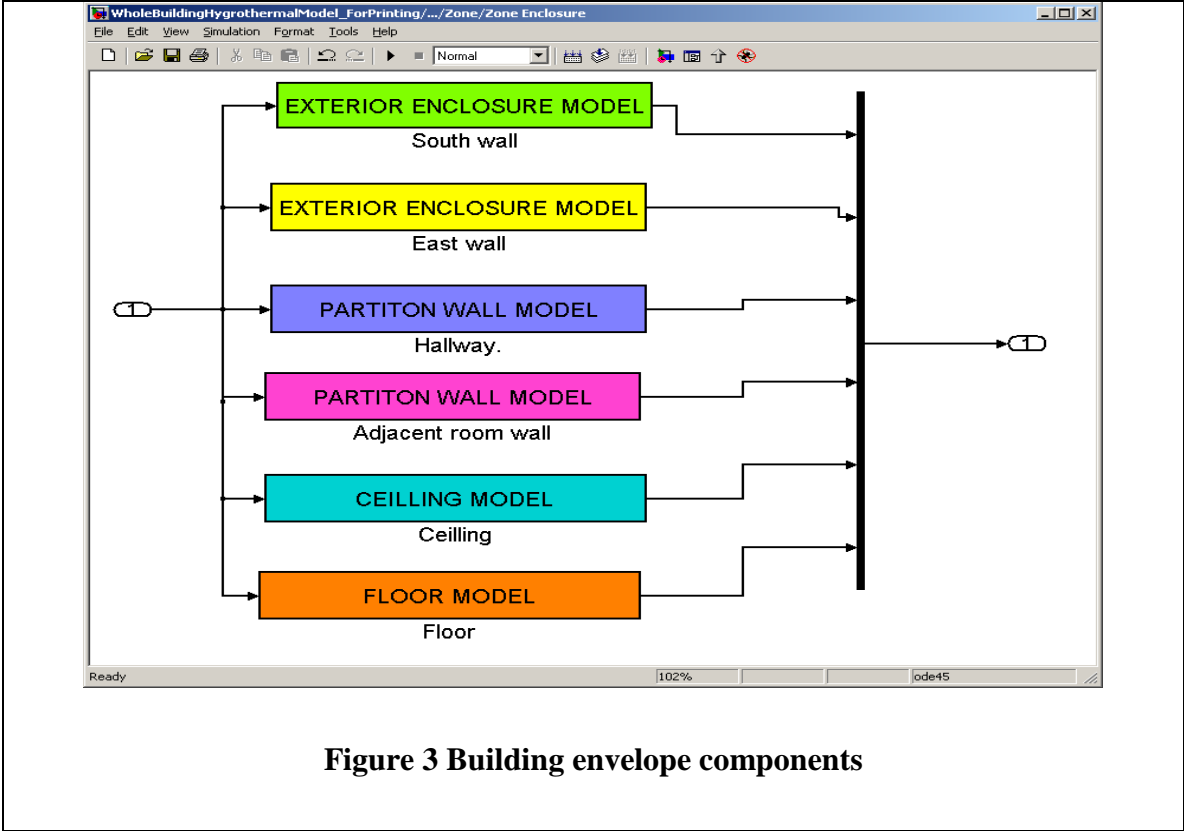


Figure 3 Building envelope components

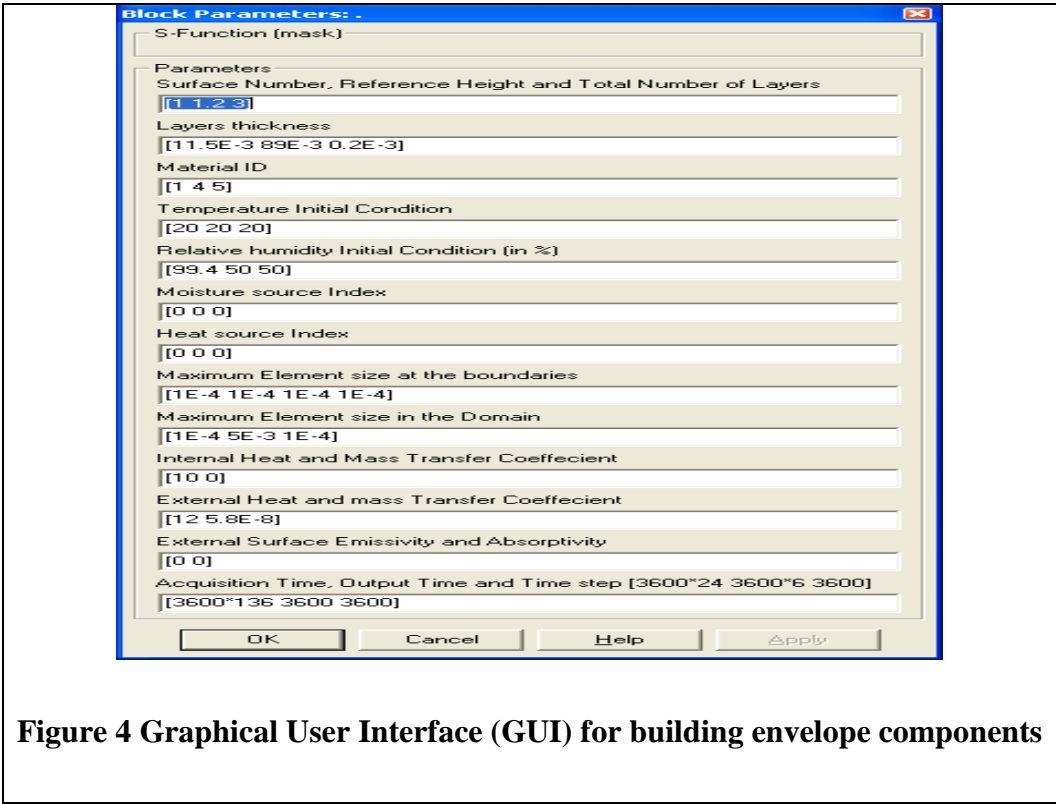


Figure 4 Graphical User Interface (GUI) for building envelope components

The “Mechanical Systems and Indoor Heat and Moisture gains” block encapsulates the mechanical systems for heating/cooling, humidification/dehumidification, ventilation, and indoor moisture and heat generation, as shown in Figure 5. The inputs of the first two blocks are indoor temperature and humidity conditions, and the corresponding outputs are the thermal (heating/cooling) and moisture (addition/removal) loads. The outputs of the blocks, which subsequently are passed to the indoor heat and moisture balance model, depend on the respective mechanical system set points and capacity. The specifications of the heating/cooling and humidification/dehumidification equipment are defined in Figure 6 and Figure 7, respectively. The third block outputs the effective ventilation rate of the house considering the combined effects of natural and mechanical ventilations. The heat and moisture loads that are independent of the indoor environment conditions (temperature and humidity) are represented in the last two blocks (examples of these loads are heat gain from light bulbs and moisture release by occupant activities). The outputs of these blocks are only a function of time and are scheduled based on assumed occupants’ daily routine activities.

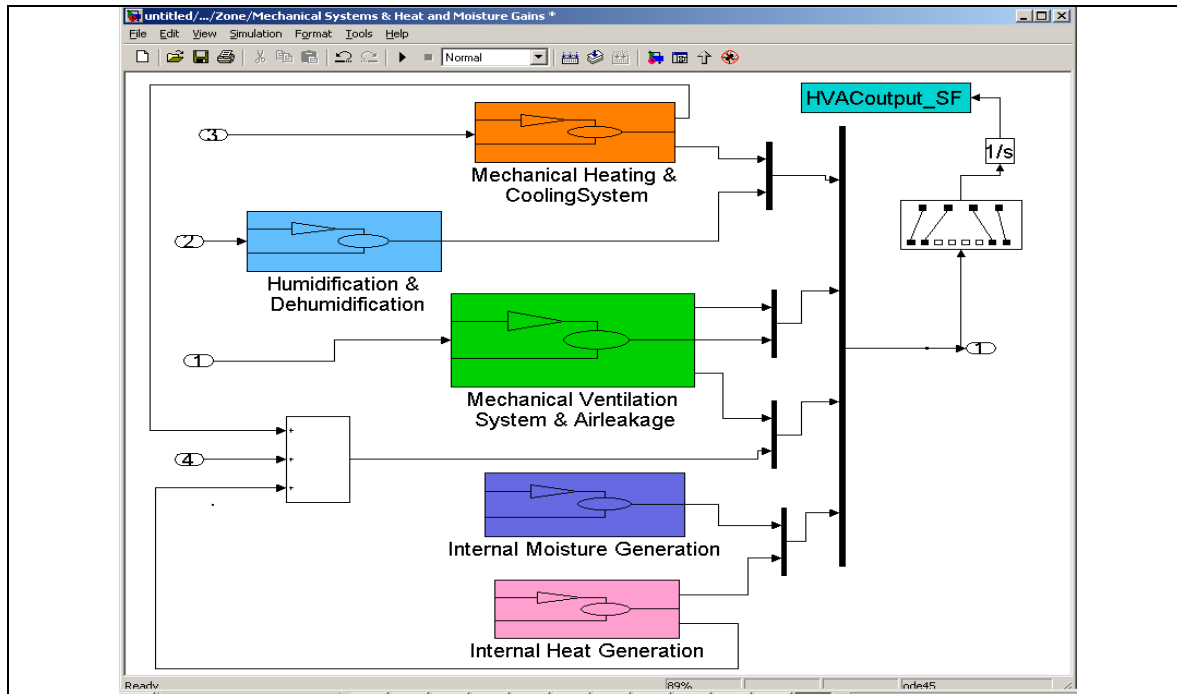


Figure 5 Mechanical Systems and Indoor Heat and Moisture gains

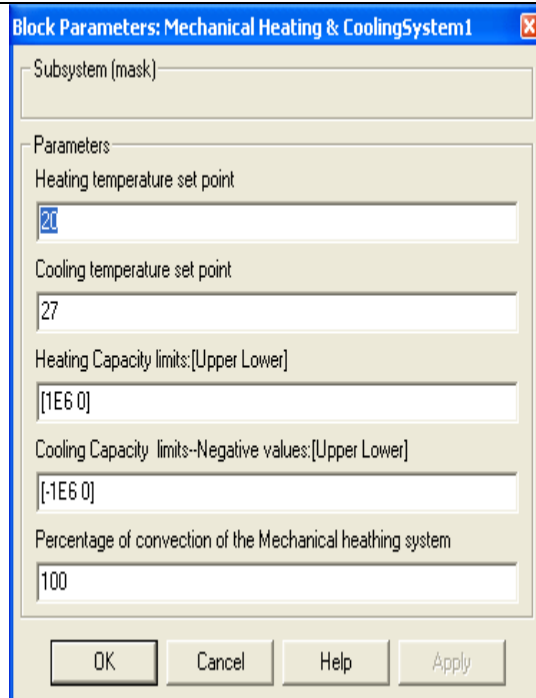


Figure 6 Heating/Cooling system GUI

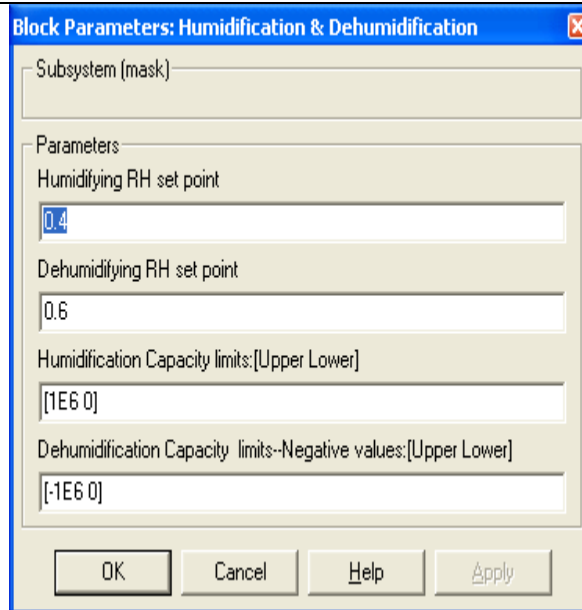


Figure 7 Humidification/Dehumidification GUI

Indoor furniture can play an important role in regulating the indoor humidity condition of the house through its moisture buffering potential. In HAMFitPlus, it is represented by “Furniture” block, Figure 2, and approximated as an interior building envelope component, whose exterior surfaces are exposed to the indoor environmental conditions. Thus, the inputs and outputs of this block are the indoor temperature and humidity conditions and the surface temperature and moisture conditions, respectively. The outputs are passed to the indoor heat and moisture balance model. The “Window” block represents one of the very important building envelope components, which is windows. The outputs of this block, which are the heat flux and window condensation rate, are used in the calculation of the humidity and energy balance of the zone. Windows in different orientations are treated independently, and their characteristics are separately specified using the GUI shown in Figure 8.

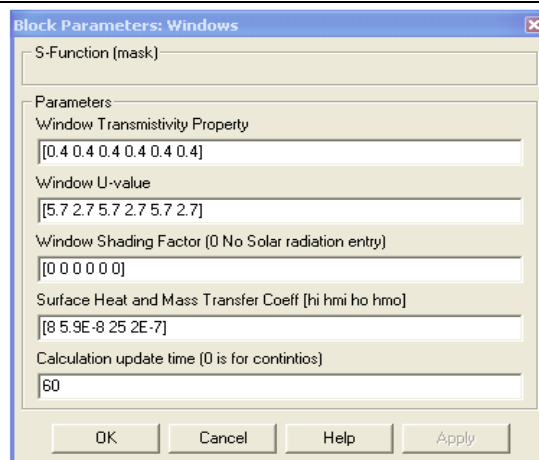


Figure 8 GUI to specify windows properties

As shown in Figure 2, the outputs of all the blocks are passed to the “Zone Humidity and Energy balance” block, which is where the two linear first-order differential equations for heat and moisture balances (Section 2.2, Equations (6) and Equations (7), respectively) are solved for the indoor temperature and humidity ratio.

The outputs of the HAMFitPlus simulation include:

- 1) Transient temperature and moisture distribution across each building envelope component
- 2) Transient indoor temperature and relative humidity conditions
- 3) Transient heating and cooling loads

Hence, the model can be used to assess building enclosure’s performance, indoor environmental conditions (temperature and relative humidity), and also energy efficiency of a building in an integrated manner.

3. INDOOR HUMIDITY MODELING OF A RESIDENTIAL HOUSE USING THE WHOLE BUILDING HYGROTHERMAL MODEL: INPUT PARAMETERS

The model is successfully verified and validated using analytical, numerical and experimental test results (Tariku, 2008; Tariku et al., 2010b). In this section, its application and implementation to predict the indoor humidity condition of an occupied dwelling is discussed. The house is located in Carmacks (Yukon Territory, Canada), and its indoor relative humidity and temperature conditions as well as the outdoor temperature and relative humidity are measured for four consecutive weeks (January 19th – February 20th) 2006. The indoor temperature and relative humidity measuring devices (HOBO Pro Series sensors) are placed in

the living room and kitchen. The complete description of the building and the survey results of the house are documented in Hood (2006) and Stad (2006). The basic input parameters of the model are: 1) building description in terms of its geometry, orientation and building site (local topography and weather conditions); 2) building enclosure, which includes building components (walls, roof, floor, windows and doors), configurations of layers of materials and their hygrothermal properties; 3) internal heat and moisture generation rates; and 4) types and capacities of mechanical systems for heating, cooling, humidification, dehumidification and ventilation. In this study, though, only heating and ventilation systems are relevant since cooling, humidification and dehumidification equipment are reportedly not present in the house. Most of the necessary input data are extracted from the survey report (Hood, 2006), and any additional input data that are required but not documented in the survey report are taken from literature. The four basic input data are discussed in detail below.

3.1. Building description

The building is a pre-engineered manufactured single detached house, which has a rectangular shape and 18° sloped roof. It is placed on a deck that is 0.914 m above ground and enclosed with OSB sheathing boards that create an unheated crawl space underneath. The house is surrounded by trees in the northeast and northwest directions. This information is important to define the wind speed profiles in the respective directions, and subsequently to calculate the air leakage rate due to wind pressure. The floor area and volume of the house are 81.9 m² and 196 m³, respectively. The floor plan of the house, Figure 9, is constructed based on the information available in the survey report such as floor area, number of bedrooms, bathrooms, windows sizes and locations, photos, and typical floor plans of manufactured houses of the same floor area that are advertised in manufacturers' websites (for example, <http://www.palmharbor.com/our->

[homes/floor-plans](#)). This information is used to estimate the interior partition wall areas that may play an active role in moisture absorption and desorption. The house is 19.5 m long and 4.2 m wide, and its front elevation is oriented toward the southwest direction. The house has two bedrooms, a living room, a kitchen and a bathroom. The total surface areas of the exterior and partition walls are 113 and 76 m², respectively. The partition wall surface area includes the surface areas of both sides of the wall since these surfaces have the same moisture buffering effect on the indoor air humidity.

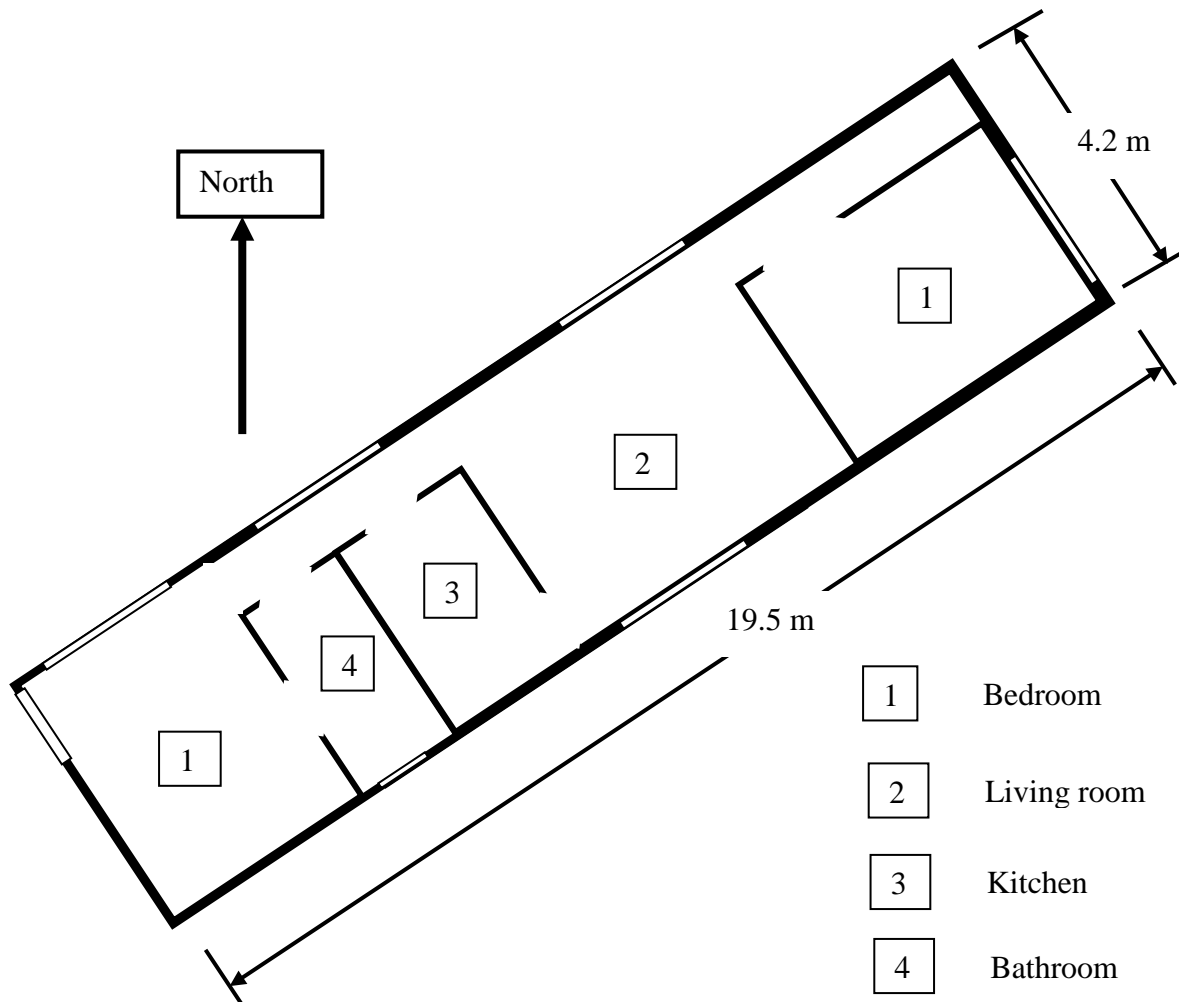


Figure 9 Floor plan and orientation of the house

3.2. Building enclosure

The house is built with a typical wood-frame construction with layers of materials to control heat, air and moisture movement through the building components. The exterior walls, floor and roof are all made of wood frame structures with layers of materials in sequence listed in Table 1 below. The wood frames of the exterior walls, floor and roof are constructed from spruce wood members measuring 2” by 6”, 2” by 8” and 2” by 4” in cross-section, respectively. The exterior wall comprises sheet metal (as a cladding material), building paper as the weather barrier, sheathing board, insulation in the stud cavity, polyethylene sheet as the vapor and air barrier and finally gypsum board as a finishing layer. The roof is protected from rain penetration into the structure with asphalt-shingles installed on top of sheathing membrane which covers the sheathing board. To control vapor flow, the vapor barrier is installed over the interior surface of the insulation. The floor is covered with linoleum tile, which is installed on top of the plywood and acts as a vapor barrier. The belly wrap (paper board), which is exposed to the crawl space, acts as an exterior sheathing layer and a weather barrier. The cavity between the floor interior sheathing board (plywood) and the belly wrap is filled with fiberglass insulation.

Table 1 Materials used for building envelope components

	Exterior Wall	Roof	Floor
Interior layer	12.5 Gypsum board	12.5 Gypsum board	12.5 Plywood
Vapor/air barrier	Polyethylene sheet	Polyethylene sheet	Linoleum tile *
Batt insulation	RSI 3.5 (m ² K/W)	RSI 7.0 (m ² K/W)	RSI 4.9 (m ² K/W)
Sheathing board	12.5 mm OSB	12.5 mm OSB	**
Weather barrier	Building paper	Building paper	**
Exterior layer	Sheet metal	Asphalt shingles	Paper board

* The tile is installed on top of plywood, ** The paper board serves as an exterior sheathing board and weather barrier

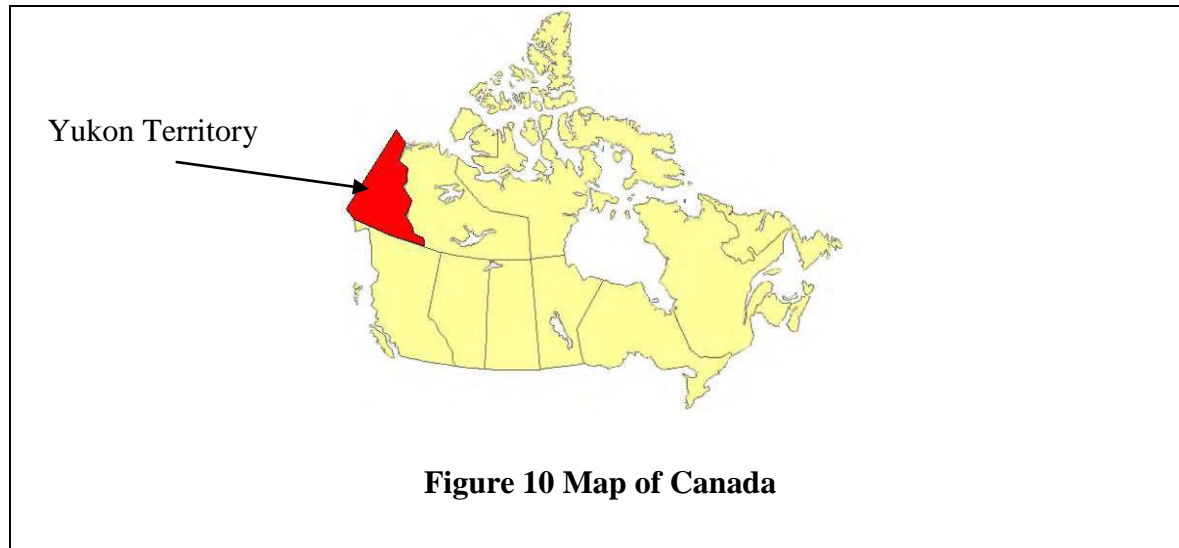
For the simulation, the hygrothermal properties of the OSB, plywood, gypsum board and insulation are taken from the ASHRAE Research Project RP-1018 '*A Thermal and Moisture Transport Database for Common Building and Insulating Materials*' (Kumaran et al., 2002). The moisture storage capacity, heat capacity, liquid permeability and thermal resistance of the membranes, linoleum tile, sheet metal and asphalt shingles are assumed to be negligible. The vapor permeability of the polyethylene sheet and building paper are taken from ASHRAE Fundamental (2009), and infinite vapor flow resistance is assumed for the linoleum tile, sheet metal and asphalt shingles. In the simulation, these materials thermal and moisture resistance properties are represented by equivalent surface transfer coefficients. The absorptivity and emissivity coefficients of the external walls are estimated to be 0.40 and 0.60, respectively, and of the roof surfaces 0.90 and 0.96, respectively. In the absence of initial condition data, the initial temperature gradients across the building envelope sections are defined based on steady state heat flow calculations using the indoor and outdoor temperatures, 20°C and -22°C. The initial moisture condition of the drywall is assumed to be the same as the moisture condition of the indoor air (33% relative humidity). The initial moisture conditions of the layers behind the polyethylene sheet are assumed to be 60% relative humidity. Since the polyethylene sheet function as a vapor barrier and the exterior cladding is sheet metal (vapor and water tight), the influence of the initial conditions of the layers behind the polyethylene sheet on the simulation result are expected to be less significant.

The house has seven windows with a total area of 15% of the floor area. The orientation and size (shown in bracket) of these windows are as follows: two windows on the southeast wall (1.58 and 0.46 m²); one window on the southwest wall (1.08 m²); three windows on the northwest wall (1.3, 1.58 and 3.72 m²) and one window on the northeast wall (2.7 m²). As reported in the survey

document, the windows are standard double-glazed windows with vinyl frame and air between the glazings. Accordingly, the overall heat transfer coefficient (U-value) and solar heat gain coefficient of the windows are assumed to be $2.87 \text{ W/m}^2\text{K}$ and 0.6, respectively (ASHRAE Fundamental, 2009). The house has two external doors (1.87 m^2 area each) that are installed on the northeast and northwest walls. It is reported that the core material of the doors is polystyrene, and the effective thermal resistance of the doors is estimated to be $0.98 \text{ m}^2\text{K/W}$.

3.3. Outdoor boundary conditions

Carmacks is located in the northwestern part of Canada in the Yukon Territory at latitude $62^\circ 7'$ north and longitude $136^\circ 11'$ west, and has an elevation of 543 m above sea level. The location of the Yukon Territory is identified in red on the map of Canada in Figure 10. In general, the weather parameters that are required for whole building hygrothermal analysis are hourly ambient temperature, relative humidity, wind speed and direction, solar radiation (global and diffusive horizontal radiation), precipitation and sky (cloud) conditions. However, for the house considered in this study, the effect of precipitation can be ignored due to the fact that the exterior layer of the house (cladding) is sheet metal and no rain absorption is possible. The weather station in Carmacks records only ambient temperature and wind conditions – wind speed and direction. The relative humidity of the ambient air is measured as part of the field monitoring tasks (Rousseau et al., 2007). Hence, the only weather parameter that needs to be estimated to carry out the whole building hygrothermal modeling is solar radiation data.



The hourly average temperature and relative humidity of the outdoor air that are imposed on the building envelope as part of the external boundary conditions are shown in Figure 11 and Figure 12, respectively. Generally, the outdoor temperature is very cold with the hourly average maximum and minimum temperatures of 6.5 and -42.2°C , respectively. The monitoring period (January 19th – February 20th) average temperature is -19.0°C . The hourly relative humidity of the ambient air varies from 45 to 95%, with an average value of 73%. About 30% of the time, the outdoor air is calm. For all other times, the wind directions are categorized into eight subsections, each subtended by a 45° angle and plotted as percentage of occurrence in Figure 13. As can be seen in the figure, the predominant wind blowing direction during the monitoring period is southeast (25%), followed by the west (18%) and northwest (17%) directions. These orientations coincide with the orientation of the largest surface areas of the house. The mean wind speed during the monitoring period is 6.7 km/hr (1.86 m/s). However, the mean wind speeds in the separate eight subsections vary from 2.3 to 11 km/hr, as shown in Figure 14. Based on these figures (Figure 13 and Figure 14) it can be said that, during the monitoring period, wind blows in the southeast direction more frequently and at higher speed than in any other direction.

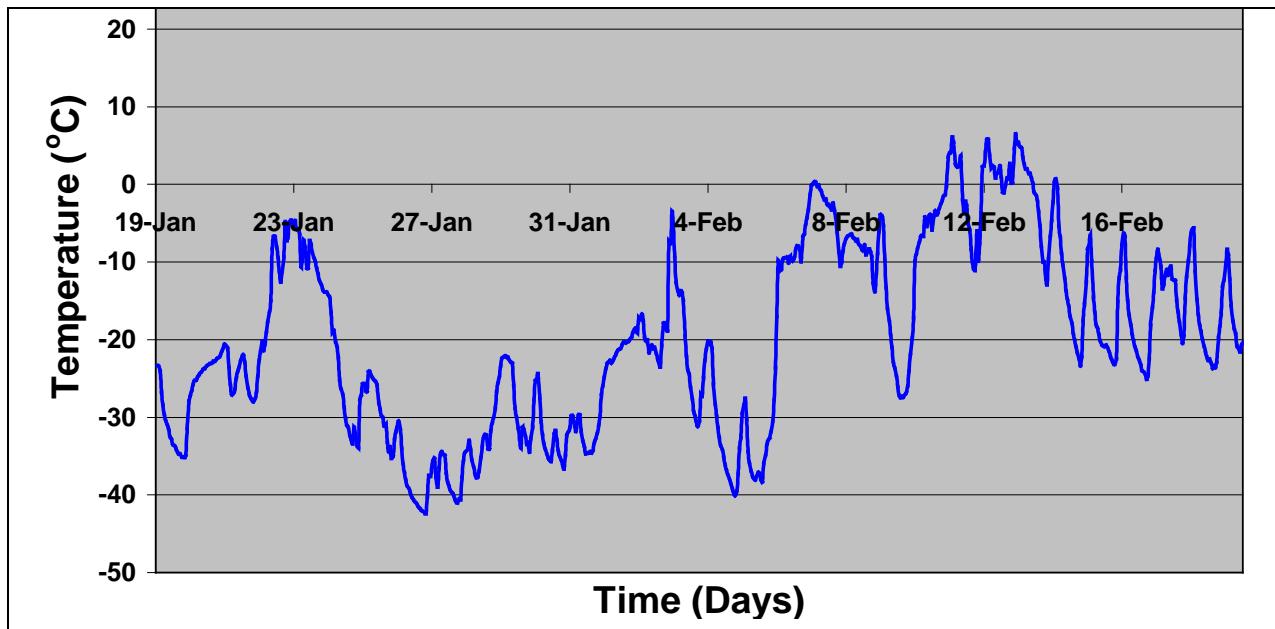


Figure 11 Hourly average temperature of Carmacks

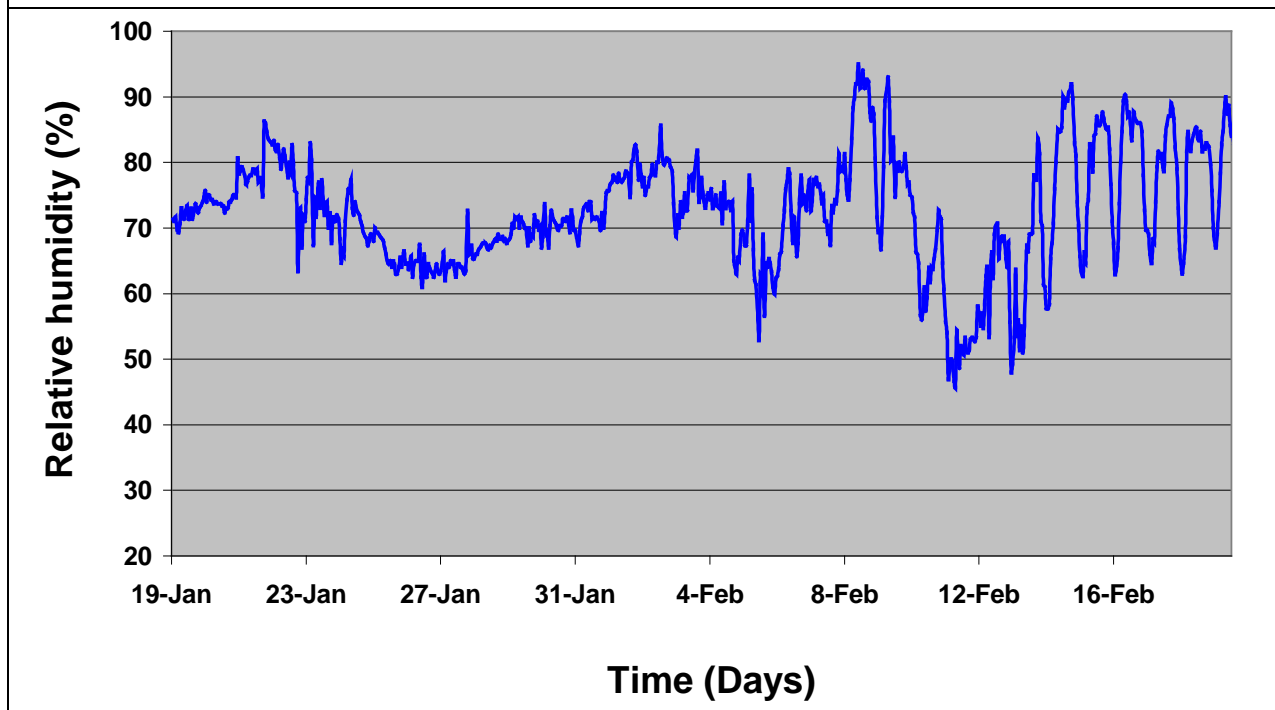
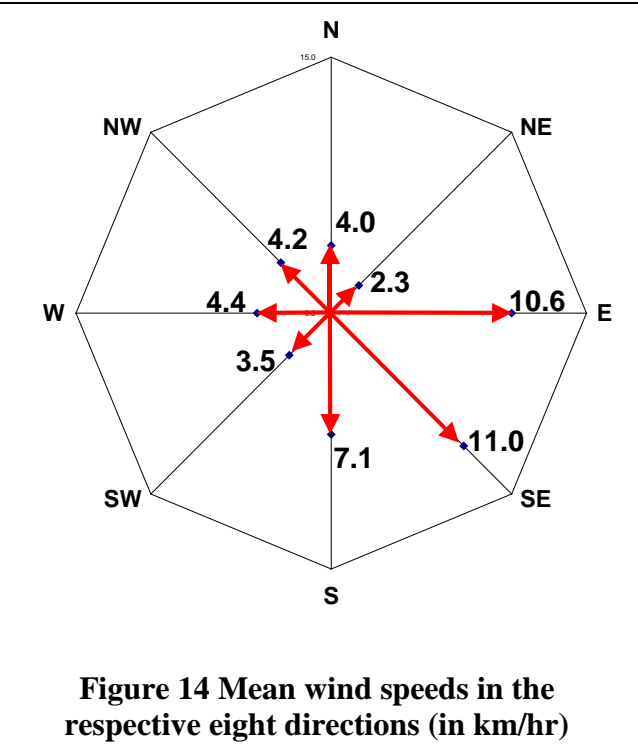
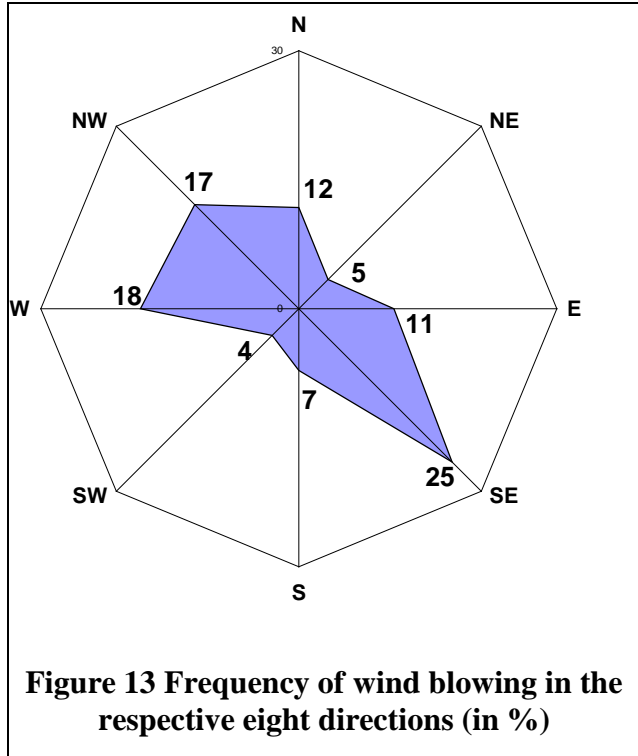


Figure 12 Hourly average relative humidity of Carmacks



The hourly horizontal global solar radiation is estimated using the Zhang and Huang solar model (2002), Equation (8). The required input data for this model include solar data (solar altitude angle and cloud cover) and other climatic conditions such as temperature, relative humidity and wind speed.

$$I_{ghz} = \left[I_{sc} \sin \beta \left\{ c_0 + c_1 CC + c_2 CC^2 + c_3 (T_n - T_{n-3}) + c_4 \phi + c_5 V_w \right\} + d \right] / k \quad (8)$$

where

I_{ghz} : Estimated hourly solar radiation in W/m^2

I_{sc} : Solar constant, $1355 W/m^2$

β : Solar altitude angle, the angle between horizontal and the line to the sun

CC : Cloud cover in tenths

ϕ : Relative humidity in %

T_n and T_{n-3} : Temperatures at hours n and n-3, respectively

V_w : Wind speed in m/s

and the correlation coefficients $c_o, c_1, c_2, c_3, c_4, c_5, d$ and k are given by:

$$\begin{aligned} c_o &= 0.5598, c_1 = 0.4982, c_2 = 0.6762, c_3 = 0.02842, \\ c_4 &= -0.00317, c_5 = 0.014, d = 17.853, k = 0.843 \end{aligned}$$

The horizontal components of the direct normal (I_{dn_hz}) and diffusive (I_{df_hz}) solar radiation are estimated from the calculated global horizontal radiation (Equation (8)) using the Watanabe et al. (1983) model, which is given by Equation (9).

$$\begin{aligned} I_{dn_hz} &= I_{sc} \sin \beta K_{DS} (1 - K_T) / (1 - K_{DS}) \\ I_{df_hz} &= I_{sc} \sin \beta (K_T - K_{DS}) / (1 - K_{DS}) \end{aligned} \quad (9)$$

where:

$$K_T = I_{ghz} / (I_{sc} \sin \beta) \quad K_{TC} = 0.4268 + 0.1934 \sin \beta$$

$$K_{DS} = K_T - (1.107 + 0.03569 \sin \beta + 1.681 \sin^2 \beta) (1 - K_T)^2, \text{ when } K_T = K_{TC}$$

$$K_{DS} = (3.996 - 3.862 \sin \beta - 1.54 \sin^2 \beta) K_T^3, \quad \text{when } K_T < K_{TC}$$

Once the horizontal components of the direct normal (I_{dn_hz}) and diffusive (I_{df_hz}) solar radiation are estimated, the solar gains of all opaque surfaces that are oriented at different

directions and inclinations, as well as indoor air space through the fenestration system, can be calculated following the procedures described in Goswami (2004).

3.4. Indoor heat and moisture gains

The house is occupied by a family of two adults and four children. The number of occupants in the daytime is five, and in the evening six. At a given time, the heat and moisture production in the house vary depending on the number of occupants and type of activities they are engaged in. The types and schedules of occupants' indoor activities in a typical day were developed based on information documented in the survey report and available in the literature. Development of hourly moisture generation of the house involved three steps: first, estimation of total daily moisture production; second, breakdown of the daily moisture production into different activities; and finally, distribution of the activities in a day. The three steps are discussed below.

Step 1: The moisture generation rate is estimated based on the data presented in ASHRAE Standard 160P (2006), Table 2. The table shows the estimated daily moisture production rates of occupants living in the same house. These rates are: 8 kg/day for 1 or 2 adults; 4 kg/day for the first child; 2 kg/day for the second child, and 1 kg/day for each additional child. Thus, the total daily moisture production of the house under consideration, based on Table 2, is estimated to be 16 kg/day.

Step 2: Christian (1994) gave the breakdown of the daily moisture production rates of a family of four (two adults and two children) due to occupants' main activities, such as dishwashing, cooking, taking showers, and respiration and perspiration of occupants (shown in Table 3). The original data, which is for a family of four, is extrapolated to a family of six to reflect the occupant size in this study. Accordingly, as presented in Table 3, the occupants

release 0.8 kg of moisture per day during dishwashing, 2.5 kg during cooking, 1.5 kg during showering, and 7.5 kg (6.25 kg in the daytime) due to respiration/perspiration. The extra moisture source (4.01 kg/day), which is the difference between the total moisture production in the house as estimated per ASHRAE Standard 160P (2006) and the sum of the extrapolated moisture production in Table 3 is assumed to be a background moisture release. This moisture source is assumed to be released constantly throughout the day, and accounts for moisture release from floor mopping, water sinks, laundry (washing and drying), plants and other unforeseen sources.

Table 2 Estimated moisture generation rates based on number of occupants

	Number of occupants	Moisture generation rate	
		L/day	g/s
1 bedroom	2	8	0.09
2 bedrooms	3	12	0.14
3 bedrooms	4	14	0.16
4 bedrooms	5	15	0.17
Additional bedrooms	+1 per bedroom	+1	+0.01

Table 3 Daily moisture productions by occupants' activities

Activity	Family of Four (kg/day)	Extrapolated for family of six (kg/day)
Dishwashing	0.5	0.80
Cooking	1.62	2.50
Shower	1	1.50
People respiration/perspiration	5	7.50 (six people) 6.25 (five people)

Step 3: Once again, to obtain the hourly moisture generation profile of the house each activity is broken-down in time, based on assumed occupants' daily routines. The schedule of activities and corresponding moisture productions in time for the assumed occupants' activities in a typical day is shown in Figure 15(a). The numbers in the boxes indicate the amount of moisture production during an activity that is carried on from the beginning to the end of the box in kilograms. In this schedule, dishwashing at breakfast, lunch and dinner preparation times is assumed to generate 0.1, 0.35 and 0.35 kg of moisture, respectively. Addition of these distributed moisture productions gives the daily total moisture production during dishwashing (0.8 kg/day), which is set in Table 3. All occupants are assumed to take showers in the morning between 6:00 and 9:00 h, and release 1.5 kg moisture (see Table 3).

Assuming light cooking in the morning compared to lunch and dinner times, the total moisture production due to cooking (2.5 kg/day) is distributed into 0.5, 0.9 and 1.1 kg, in the respective periods. The moisture production by occupants due to respiration and perspiration between 9:00 and 17:00 h (when the number of occupants is five) is assumed to be 2.08 kg ($6.25 \text{ kg/day} \times 1/3 \text{ day}$), and 5 kg for the rest of the time (when the number of occupants is six). The background moisture production (4.01 kg), which accounts for all the unknown moisture sources, is uniformly spread over a 24-hour duration. Finally, the constructed diurnal moisture generation schedule looks like the one in Figure 15(b). The maximum moisture generation (1184 g/hr) occurs during the morning period between 6:00 and 9:00 h, followed by dinnertime (17:00-20:00 h) at the rate of 968 g/hr. The occupants are assumed to be at rest from 13:00 to 17:00 h (after lunch until the time to prepare dinner), and consequently, the moisture generation rate during this period is the lowest (432 g/hr). The diurnal heat generation schedule shown in Figure 16(a) is formulated in the same fashion as the moisture production rate, which is based on assumed

occupants' daily routines. This information is specifically important for simulation cases where the indoor temperature and energy demand are computed. In Figure 16(a) the numbers in the boxes indicate the heat generation during an activity that is carried on from the beginning to the end of the box in Watt-hour. Occupants are one of the heat sources that can raise the indoor temperature. In this work, the sensible heat gain from an occupant is taken as 67 W, which is adopted from Athienitis and Satamouris (2002). Assuming constant and equal heat release rates for all occupants, the total sensible heat gains during 9:00 to 17:00 h (five occupants) and at all other times (six occupants) are taken as 335 W and 402 W, respectively. The periodic heat source that is associated with cooking can significantly raise the indoor temperature as well. The corresponding heat releases to the indoor air space during breakfast (6:00-9:00 h), lunch (9:00-13:00 h) and dinner (17:00-20:00 h) preparations times are to be approximated at 750, 2000 and 2000 Watt-hour, respectively. Moreover, the family is assumed to use a computer between lunch and dinnertime (13:00-17:00 h), whose heat generation rate is to be approximated at 125 W (ASHRAE Fundamental, 2009). During the evening (17:00-23:00 h), lighting and entertainment appliances such as television are assumed to generate an additional heat gain of 350 W. Assembling these heat generation items yields a typical diurnal heat generation schedule for the house under consideration, Figure 16(b). As shown in the figure, the lowest heat generation rate (402 Watts) occurs during sleeping time (23:00-6:00 h next morning), and the maximum (1419 Watts) during dinnertime (17:00-20:00 h). In the HAMFitPlus simulations, the internal heat gain at a time is assumed to be composed of 50% radiative and 50% convective heat gains. The radiative heat gain is uniformly distributed and applied on the building envelope interior surfaces as radiative heat flux.

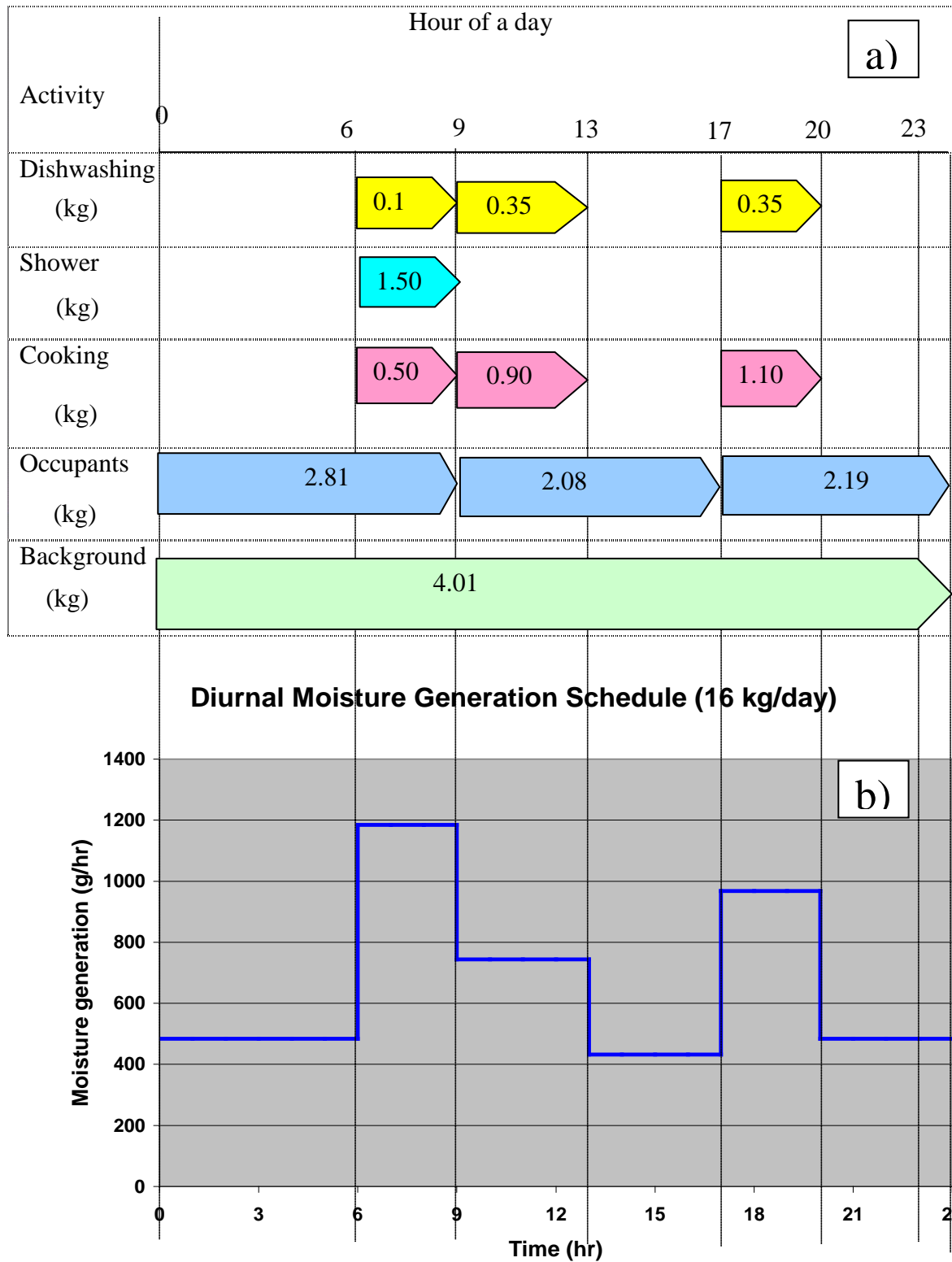


Figure 15 Development of a daily moisture generation profile. a) schedule of activities and corresponding moisture productions in time, b) moisture generation profile of a typical day

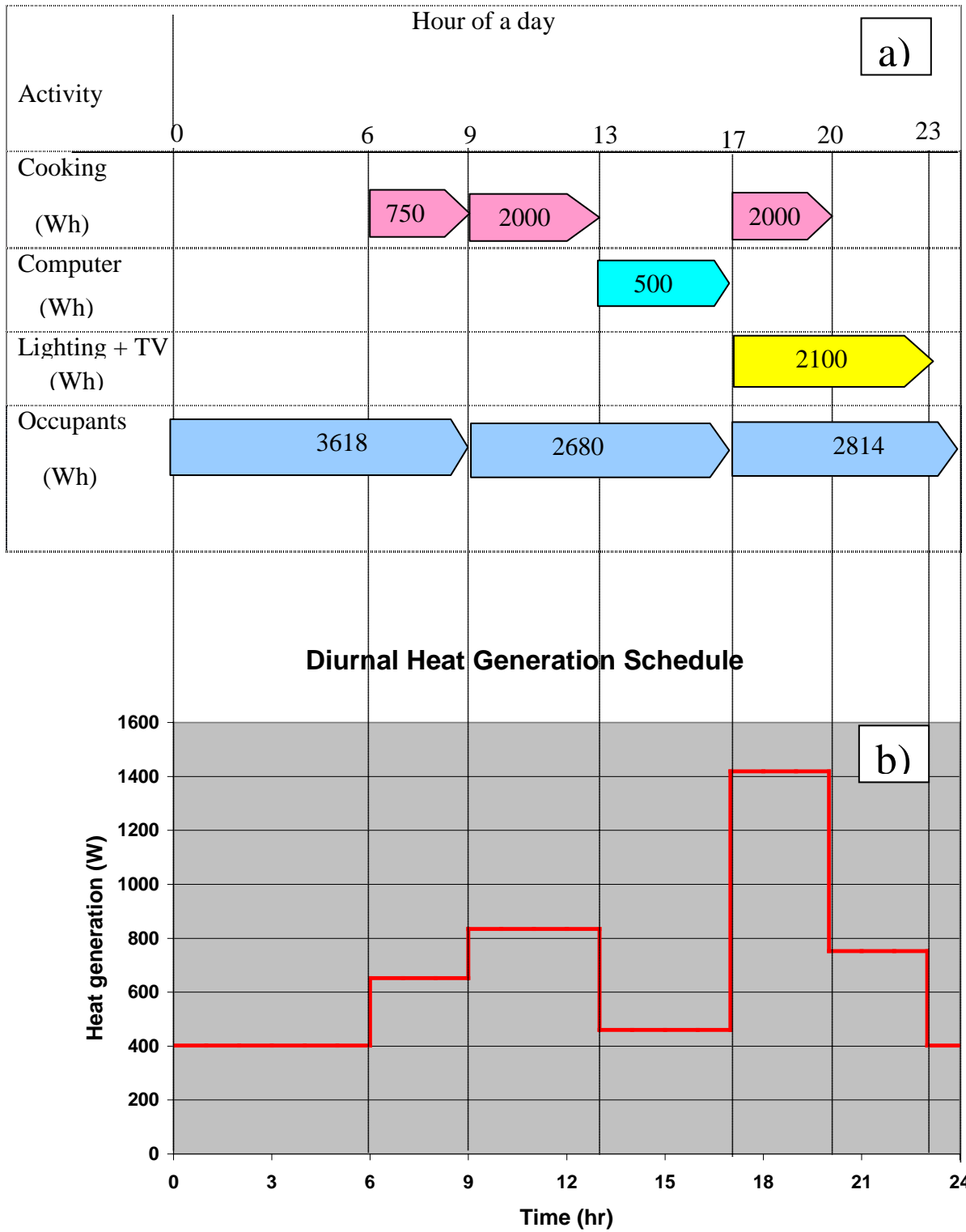


Figure 16 Development of a daily heat generation profile. a) schedule of activities and corresponding heat gains in time, b) heat generation profile of a typical day

3.5. Mechanical systems

The house is equipped with a mechanical heating system, which consists of an oil-fired furnace and forced-air heat distribution system (fan and ducts). The actual heating capacity of the heating system is not reported in the survey document, but the measured indoor air temperature of the house during the monitoring period suggests that the system has enough heating capacity to maintain the indoor air temperature at $20^{\circ}\text{C} \pm 2^{\circ}\text{C}$. Subsequently, an infinite heating capacity is assumed for HAMFitPlus simulations. The house also has a mechanical ventilation system, more specifically exhaust fans. The fans are installed in the bathrooms and kitchen. However, as the surveyor reported, they are not usually operational due to malfunction or kept turned-off to avoid the noise that is generated during their operation. Consequently, for the house under consideration, natural ventilation is the only means of ventilation whereby air exchanges take place through unintended openings (airleakage) and/or through intentional openings (e.g., window openings). For the simulation period considered in this study, that is, when the outdoor temperature is very cold and opening of windows is impractical, the natural ventilation is assumed to occur only by airleakage.

The air exchange rate due to the time-varying wind and stack pressure is calculated using a simple single zone infiltration model. The model is developed based on conservation of mass (i.e., the total mass flow rates of infiltrated and exfiltrated air across the building envelope are equal), as outlined in Hutcheon and Handegord (1995). Application of the infiltration model involves determination of: the neutral pressure level (to compute the stack pressure at any given height of the building envelope component), the local wind speed, the surface pressure coefficients, and the airleakage coefficients of building envelope components, and finally, solving the nine nonlinear equations simultaneously (two for each exterior walls and one for the

roof). The wind pressure at the surfaces of the four walls and roof are determined from the local wind velocity profile and wind pressure coefficient of the respective surface. The wind pressure coefficient for a surface depends on the angle between the line perpendicular to the surface and the wind direction (Orme et al., 1998). Except for the determination of the airleakage coefficients of the building envelope components, which need to be defined once, all the other steps are repeated whenever the wind or the temperature conditions change.

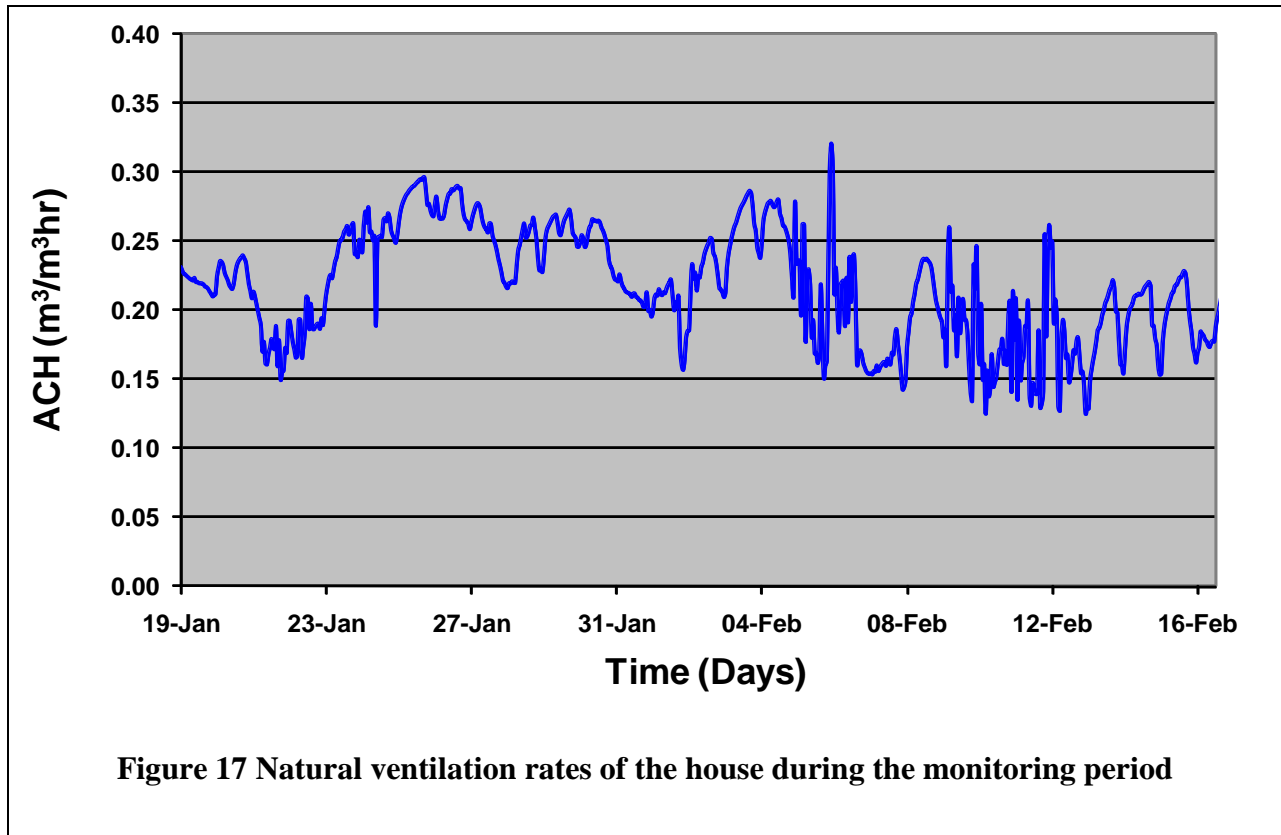
The air leakage characteristics of the building envelope components (walls and roof) are determined using the air-tightness test result of the whole house (Hood, 2006). The measured total airleakge rate of the house at 50 Pa depressurization is 5.04 ACH (air exchange per hour), which is equivalent to 0.2744 m³/h. In this work, for lack of better data, it is assumed that two-thirds of the total airleakage is through the exterior walls and the rest through the roof. The floor is assumed to be airtight based on the fact that its top and bottom layers are airtight. Subsequently, the proportion of airleakages through the exterior walls and roof are 3.36 ACH (0.1829 m³/hr) and 1.68 ACH (0.0915 m³/hr), respectively, and the airleakage coefficients of the respective building envelope components, as calculated using Equation [10] (Hutcheon and Handegord, 1995), are 1.4595E-4 kg/s.m².Pa^{0.67} and 9.7302E-05 kg/s.m².Pa^{0.67}, respectively.

$$Q_a^v = A \times C \times \Delta P^n \quad [10]$$

where: Q_a^v is the airleakage rate (kg/s), A is the airleakage area (m²), C is the airleakage coefficient (kg/s.m².Paⁿ), ΔP is the pressure difference across the building envelope component (Pa) and n is the flow exponent (dimensionless).

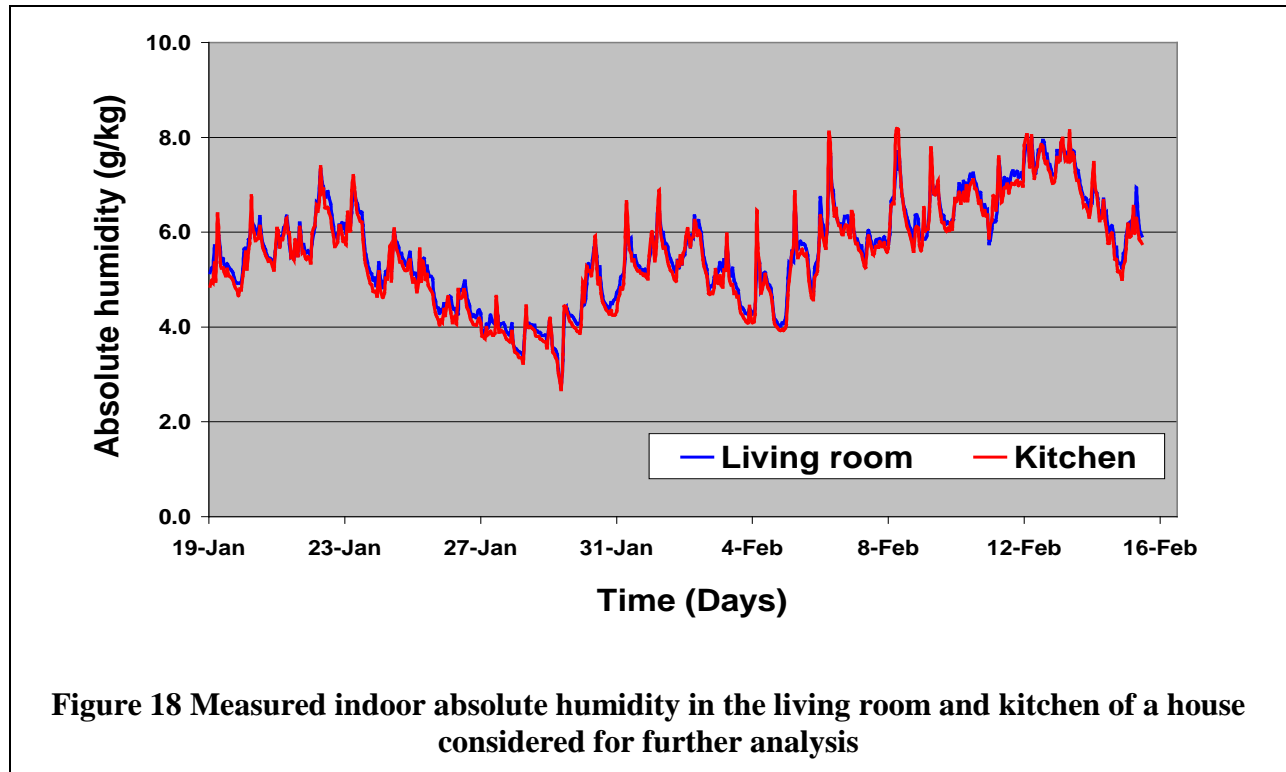
Figure 17 shows the calculated natural ventilation rates of the house during the monitoring period. During this period, the airleakage rate varies from 0.13 to 0.34 ACH, while the average is

0.23 ACH. In the simulation case considered here, where the indoor temperature is nearly stable and the weather data is hourly, the air exchange rate computations are done hourly.



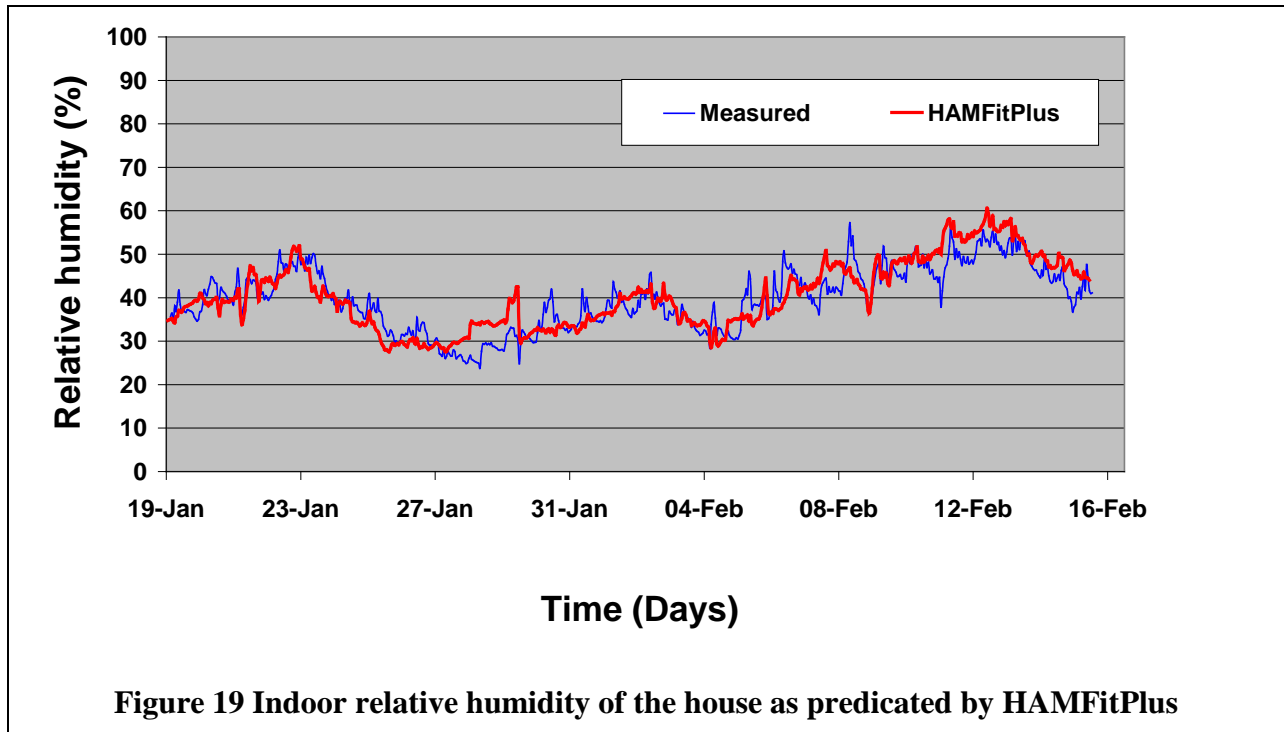
4. INDOOR HUMIDITY SIMULATION OF THE HOUSE UNDER CONSIDERATION

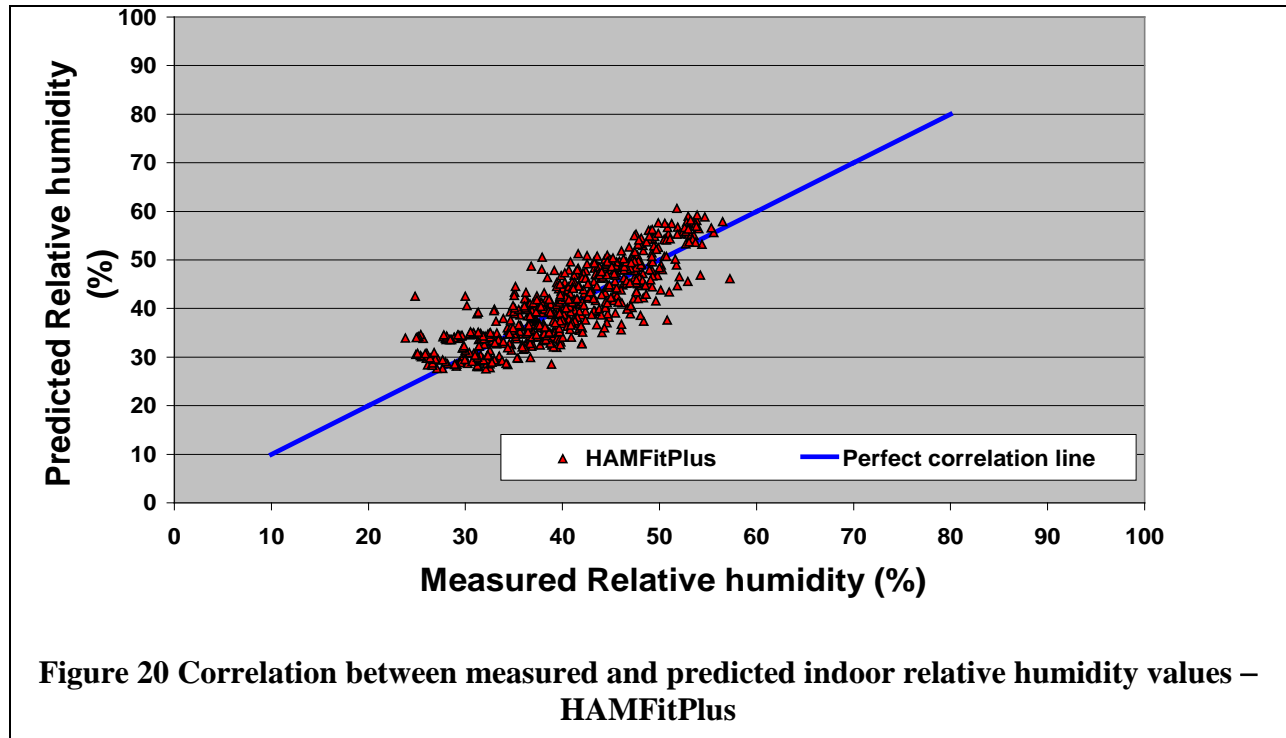
The moisture distribution in the indoor air is fairly uniform, which is attributed to the relatively small size (81.0 m^2) of the house and the air distribution system that results in air mixing. Figure 18 presents the measured absolute humidity of the indoor air at two locations, living room and kitchen. As the data indicate, the house has uniform indoor environmental conditions and can be represented in the whole-building simulation as a single zone.



The indoor humidity simulation result of the house, using the input parameters discussed in Section 3, is shown in Figure 19 along with the measured data. The simulation, which took about 20 minutes runtime, is carried out on a computer with Quad-Core Intel Xeon Processor (3.00 GHZ) and 3.00 GB Ram, and software versions of COMSOL Multiphysics 3.5a and MatLab 7.7. In general, the HAMFitPlus simulation results are in good agreement with the measured data. The mean predicted indoor relative humidity values of the HAMFitPlus model (40.5%) are close to the corresponding mean measured value (39.8%). Moreover, the highest and lowest predicted mean relative humidity values (27.6 and 60.6%, respectively) are close to the corresponding measured values (23.8 and 57.3%, respectively). The correlations between the indoor relative humidity measurement and simulation results are presented graphically in Figure 20. The blue line in the figures represents an ideal case where the measured and predicted values are in perfect agreement. The closer the data plot to this line, the more accurate is the prediction of indoor

relative humidity obtained by the model. As shown in Figure 20, most of the data are very close to the perfect-correlation line. For almost half (49.47%) of the simulation period, the relative humidity difference between the measured and HAMFitPlus predicted values (absolute errors) is less than 3% (relative humidity), while for 77.54% (nearly three-quarter) of the simulation period, the relative humidity difference is below 5% (relative humidity). For nearly the entire simulation period (98.18%), the absolute errors are less than 10% (relative humidity). Thus, the indoor humidity simulation result of HAMFitPlus can be considered as satisfactory.





The average indoor relative humidity for the monitoring period is 39.8%, while the hourly values can vary from the lowest value of 23.8% to the maximum value of 57.3%. The indoor relative humidity decreases from about 50% to 23.8% between January 23 and January 28. During the same period, the outdoor temperature decreases from -4 to -40°C (Figure 11), which results in an increase in stack pressure due to the increase in temperature differences between the indoor and outdoor air. The increased stack pressure resulted in a higher airleakage rate, as shown in Figure 17. Since the moisture content of the outdoor air during this period (low temperature) is insignificant, the high airleakage rate takes away more moisture than it brings into the indoor space, resulting in decreasing relative humidity, as shown in Figure 19. A relatively high indoor relative humidity level is observed in the second week of February. During this period the outdoor temperature is relatively higher, which results in low ventilation. In general, for the house and climate considered in this study, the outdoor temperature plays a major role in

regulating the indoor humidity conditions through its predominant effect on stack pressure and, thereby, ventilation. A lower humidity level is expected during very cold outdoor temperatures (due to enhanced stack-effect - ventilation) and a relatively higher humidity in cold outdoor temperature conditions (minimized stack-effect-ventilation). Thus, problems associated with high indoor humidity such as mold growth and degradation of building envelope components can be expected during warm winter periods (early or late periods of winter). In other words, a weather condition that does not permit enough natural ventilation by opening windows as is the case in summer, or that creates high natural ventilation due to very cold outdoor temperatures (stack pressure), may pose problems.

To assess the effect of building envelope components on indoor humidity, an additional HAMFitPlus simulation is carried out without taking into account the moisture buffering effect of the interior furnishing of the building envelope components. As can be seen in Figure 21, the deviation of the simulation and measured data is pronounced at times when the ventilation rate is low and the indoor humidity is relatively high. The only difference between the simulation cases whose results are shown in Figure 19 and Figure 21 is the inclusion or exclusion of moisture buffering effects of materials, and consequently the higher deviations observed in Figure 21 must be due to the absence of moisture absorption/desorption effects of building envelope components. In the simulation case with no moisture buffering, the indoor humidity reaches as high as 78% (on February 13th) compared to the 60% that is calculated when moisture buffering effect is considered. Thus, incorporation of moisture buffering effects of materials in indoor humidity modeling is very important to accurately predict the indoor humidity condition of a building, especially for cases where the indoor humidity is expected to be higher.

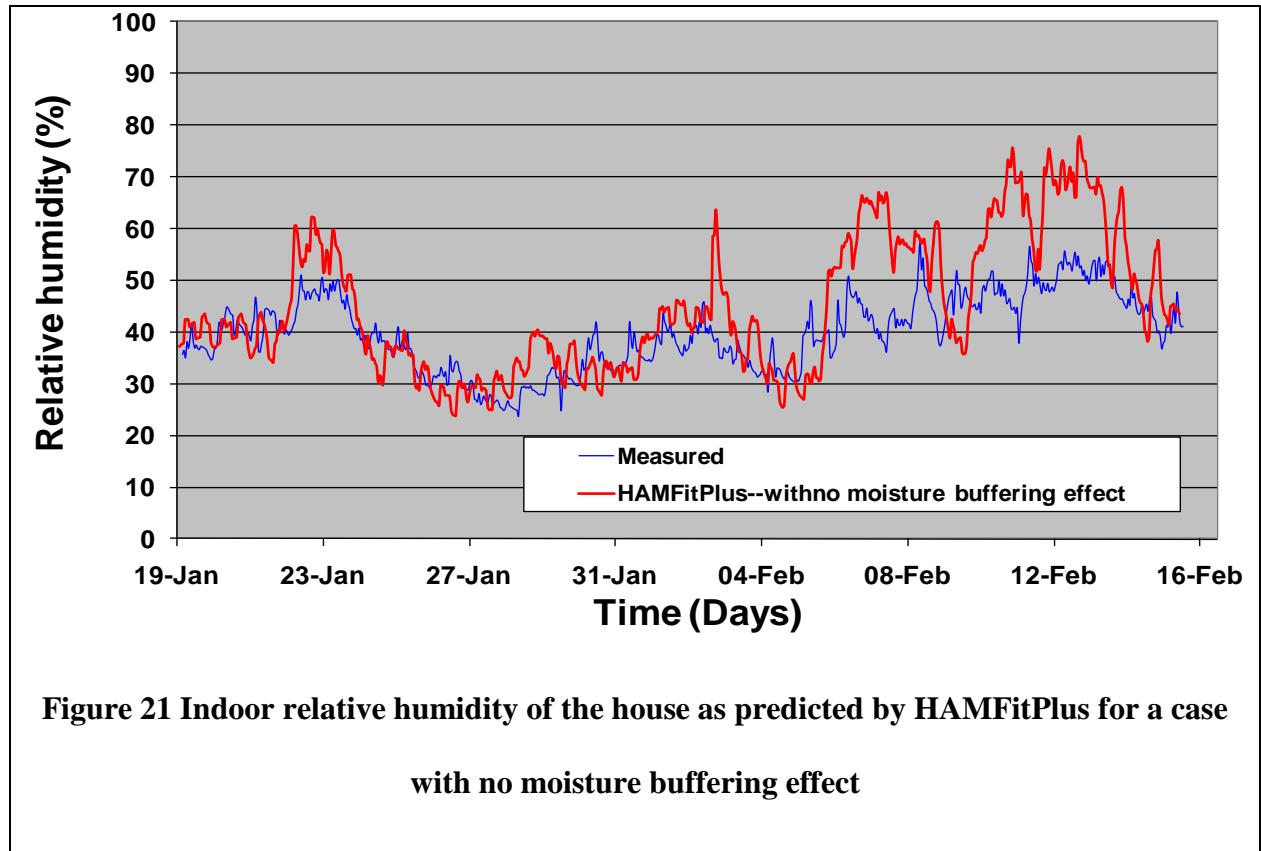


Figure 21 Indoor relative humidity of the house as predicted by HAMFitPlus for a case with no moisture buffering effect

Like the moisture buffering effects of the interior finishing of the building envelope components, it is important also to consider the phenomenon of moisture removal from the indoor air due to condensation on window surfaces, and subsequent evaporation of the condensate to the indoor air. In the house considered in this paper, a significant amount of moisture condenses and freezes on windows due to the fact that the indoor moisture source is relatively high for the size of the house and also the outdoor temperature is low. The surveyor (Stad, 2006) reported considerable condensation on windows and ice buildup as shown in Figure 22, and also moisture staining and possible deterioration of the lower portion of the walls below windows. Indoor humidity simulation of the house without considering the effect of windows and the moisture buffering effect of building envelope components results in a very highly elevated and unrealistic indoor

humidity profile as shown in Figure 23, where the minimum relative humidity is 61% and the maximum is 100%.



Figure 22 Excessive window condensation (Stad 2006)

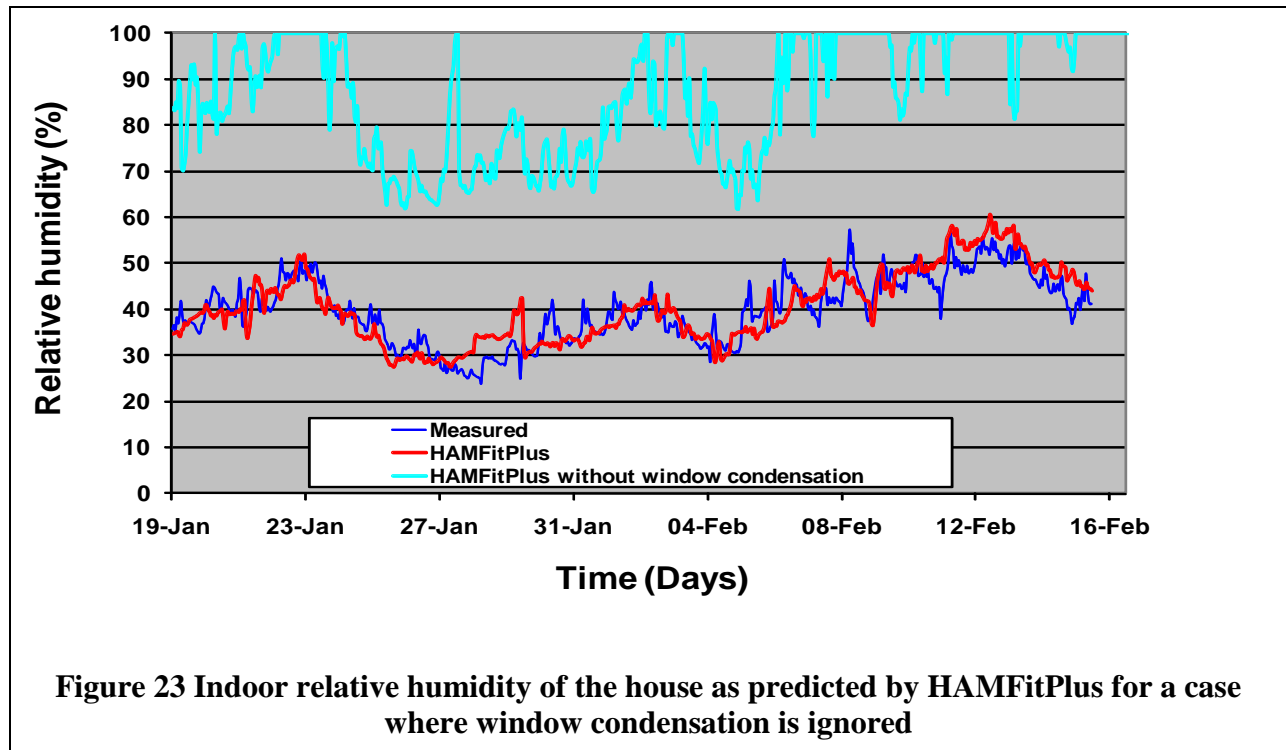


Table 4 summarizes the indoor humidity predictions of the house using an empirical model, Class model (Sandberg, 1995), and a steady-state model, ASHRAE Standard 160 Intermediate model.

Table 4 Statistical summary of the indoor relative humidity values obtained from measurements and numerical models.

	Measured values (%)	CLASS Model (%)	ASHRAE Standard 160P Intermediate (%)	HAMFitPlus (%)
Mean	39.8	51.7	86.5	40.5
Minimum	23.8	46.4	61.8	27.6
Maximum	57.3	70.7	100.0	60.6

As shown in the table, the indoor humidity predictions obtained from the simplified indoor models and HAMFitPlus varies significantly. The mean, minimum and maximum predicted indoor relative humidity values of the HAMFitPlus are close to the corresponding measured values. In the cases of the simplified models, the ASHRAE Standard 160P Intermediate model and the Class model, however, the mean, minimum and maximum predicted values are relatively high compared to the experimental values. Thus, it is important to take into account the dynamic interactions between the building envelope and the indoor environment in detail, as the case with the HAMFitPlus simulation, to obtain a good prediction of indoor humidity conditions and building envelope durability.

5. CONCLUSION

To assess the indoor humidity condition of a new building design or retrofit of an existing building, it is important to use a model that takes into account the dynamic interactions of building envelope components and indoor environments. The model that is presented in this paper treats the house as a system and considers the specific features of the house including orientation, the building materials used, occupant density and assumed activities. In general, the HAMFitPlus simulation results are in good agreement with the measured data. Application of empirical or steady state humidity models, which do not incorporate the transient nature of moisture buffering effects and also the various moisture sources and removal mechanisms including window condensation and construction moisture, need to be limited to first order approximation. In some cases, these models can give unrealistic indoor humidity profiles as presented in the simulation case where window condensation is omitted (which is the case with the ASHRAE 160P Intermediate humidity model).

The moisture buffering effect of the interior layer of the building envelope components helps to modulate the indoor humidity of the house. Its effect is prominent at times when the indoor air has a potential to have high humidity, either due to high indoor moisture production or reduced ventilation. The measured and simulated results indicate that high indoor humidity conditions occur when the outdoor temperature is relatively warm. In mild weather conditions, including late fall and early spring seasons, it is beneficial to have a mechanical ventilation system that supplements the reduced stack-effect natural ventilation to avoid building envelope damage and occupants' health risk related to elevated indoor humidity.

6. ACKNOWLEDGEMENTS

The authors would like to acknowledge Dr. Wahid Maref, Ms. Madeleine Rousseau, Mr. Steve Cornick and Dr. Nadi Said for kindly sharing the building survey and experimental data with us.

7. REFERENCES

- Abranties, V; Freitas, V. (1989). User Influence Upon Building Indoor Humidity, *Housing Science*, Vol. 13 (4) pp 277-282
- Athenatis, A.; Santamouris, M. (2002). Thermal Analysis and Design of Passive Solar Buildings. *Published by James & James* (science Publishers) Ltd., London, UK, ISBN 1-902916-02-6
- ASHRAE Standard 60P. (2006). Design Criteria for Moisture Control in Buildings.
- ASHRAE Handbook of Fundamentals (2009). American Society of Heating, Refrigeration, and Air-Conditioning Engineers, Atlanta
- Christian, J.E. (1994). Moisture Sources. Moisture Control in Buildings, ASTM Manual Series: MNL 18, pp. 176-182.
- Clausen, G.; Rode, C.; Bornehag, C.-G.; Sundell, J. (1999). Dampness in Buildings and Health. Interdisciplinary Research at the National Center for Indoor Environment and Energy. *Proceeding of the 5th Symposium of Building Physics in The Nordic Countries*
- Diasty, R.; Fazio, P.; Budaiwi, I. (1992). Modelling of Indoor Air Humidity: The Dynamic Behaviour with in Enclosure. *Energy and Buildings*, Vol. 19, pp.61-73
- Diasty, R.; Fazio, P.; Budaiwi, I. (1993). The Dynamic Modeling Air Humidity Behavior in a Multi-Zone Space. *Building and Environment*, Vol. 28, pp.33-55
- Fang, L. Clausen, G and Fanger, P.O. (1998a). Impact of Temperature and Humidity on the Perception of Indoor Air Quality, *Indoor Air*, Vol. 8, pp. 80-90.
- Fang, L. Clausen, G and Fanger, P.O. (1998b). Impact of Temperature and Humidity on the Perception of Indoor Air Quality During and Longer Whole-Body Exposures, *Indoor Air*, Vol. 8, pp. 276-284.
- Goswami, D. (2004). Energy Resources: Solar energy resources, *The CRC Handbook of Mechanical Engineering*, 2nd Edition, ISBN13: 9780849308666, Publisher CRC

- Hood, I. (2006). Field Survey of Indoor and Outdoor Climatic Conditions and Airtightness Level Prevailing in Two Northern Housing Regions, *Status Report: Carmacks Survey*, Report submitted to NRC-IRC, Vancouver
- Hutcheon, N.; Handegord, G. (1995). Chapter 12: Water and Buildings, *Building Science for a Cold Climate*, National Research Council of Canada
- Jones, R. (1993). Modeling Water Vapor Conditions in Buildings. *Building Services Engineering Research and Technology*, Vol. 14 (3), pp.99-106.
- Jones, R. (1995). Indoor Humidity Calculation Procedures. *Building Services Engineering Research and Technology*, Vol. 16 (3), pp.119-126
- Kumaran, K.; Lackey, J.; Normandin, N.; Tariku, F.; van Reenen, D. (2002). A Thermal and Moisture Transport Property Database for Common Building and Insulating Materials, *Final Report—ASHRAE Research Project 1018-RP*, pp.229
- Kumaran, M.K. (2005). Indoor Humidity as a Boundary Condition for Whole Building HAM Analysis. *Annex 41 Working Document*, A41-T3-C-05-1
- Kusuda, T. (1983). Indoor Humidity Calculations, *ASHRAE Transactions*, DC-83-12
- Loudon, A.G. (1971). The Effect of Ventilation and Building Design Factors on the Risk of Condensation and Mould Growth in Dwellings. *The Architects' Journal*, Vol. 153 (20), pp. 1149-1159
- Orme, M.; Liddament, W. (1998). Numerical data for air infiltration and natural ventilation calculations- Table 3.5. *AIVC TN 44*, pp.100.
- Oreszczyn, T.; Pretlove, S. (1999). Condensation Targeter II: Modeling surface relative humidity to predict mould growth in dwellings. *Proceeding CIBSE: Building Services Engineering Research and Technology*, Vol.20 (3), pp. 143-153.
- Rode, C. (2003). Whole Building Hygrothermal Simulation Model. *ASHRAE Transactions*:
- Rousseau, M., M. Manning, M.N. Said, S.M. Cornick, and M.C. Swinton (2007), “Characterization of Indoor Hygrothermal Conditions in Houses in Different Northern Climates”, *Thermal Performance of the Exterior Envelopes of Whole Buildings X International Conference*, Clearwater Beach, FL, pp. 14, Dec. 2-7.
- Sandberg, P.J. (1995). Building Components and Building Elements—Calculation of Surface Temperature to Avoid Critical Surface Humidity and Calculation of Interstitial Condensation. *Draft European Standard CEN/TC 89/W 10 N 107*

- Schijndel, A.W.M; Hensen J.L.M. (2005). Integrated Heat, Air and Moisture Modeling Toolkit in MatLab. *Proceeding of the ninth International IBPSA Conference*. August 15-18, Montreal, Canada, pp 1107-1113.
- Stad, T. (2006). Energuide and Condition Report Summary, Report submitted to NRC-IRC, Carmacks, Yukon, pp 16
- Sterling, E.M.; Arundel, A.; Sterling, T.D. (1985). Criteria for human exposure to humidity in occupied buildings. *ASHRAE Transactions*, 91 (1B)
- Tariku, F. (2008). Whole Building Heat and Moisture Analysis. *Ph.D. Thesis*. Concordia University, Montreal, Canada.
- Tariku, F.; Kumaran, M.K.; Fazio, P. (2009). The need for an accurate indoor humidity model for building envelope performance analysis. *4th International Building Physics Conference*, Istanbul, Turkey, June.15-18, 2009.
- Tariku, F.; Kumaran, M.K.; Fazio, P. (2010a). Transient Model for Coupled Heat, Air and Moisture Transfer through Multilayered Porous Media. *International Journal of Heat and Mass transfer*. Vol. 53 (15-16), pp 3035-3044.
- Tariku, F.; Kumaran, M.K.; Fazio, P. (2010b). Integrated Analysis of Whole-Building Heat, Air and Moisture Transfer. *International Journal of Heat and Mass transfer*. Vol. 53 (15-16), pp 3111-3120.
- TenWolde, A. (1988). Mathematical Model for Indoor Humidity in Houses during Winter, *Proceedings of Symposium on Air Infiltration, Ventilation and Moisture Transfer*, Washington DC: Building Thermal Envelope Coordinating Council.
- TenWolde, A. (1994). Ventilation, Humidity, and Condensation in Manufactured Houses During Winter. *ASHRAE Transactions*, 100(t): 103-115
- TenWolde, A. (2001). Interior Moisture Design Loads for Residences. *Building VIII: Performance of exterior envelopes of whole buildings*. Dec. 2-7, Clearwater, FL
- Toftum, J.; Fanger, P.O. (1998). Air Humidity Requirements for Human Comfort. *ASHRAE Transactions*, Vol. 105 (2), pp 641-647.
- Trechsel, H.R. (2001). Moisture Primer, *Moisture Analysis and Condensation Control in Building Envelopes*, ASTM Manual series 50: Chapter 1
- Tsongas, G.; Burch, D.; Roos, C.; Cunningham, M. (1996). A Parametric Study of Wall Moisture Contents Using a Revised Variable Indoor Relative Humidity Version of the

MOIST Transient Heat and Moisture Transfer Model. *Proceedings of the Thermal Performance of Exterior Envelopes VI Conference*, Dec. 4-8, Clearwater Beach, FL

Watanabe, T.; Urano, Y.; Hayashi, T. (1983). Procedures for Separating Direct and Diffuse Isolation on a Horizontal Surface and Prediction of Isolation on Tilted Surfaces. Transactions, No. 330, *Architectural Institute of Japan*, Tokyo, Japan.

Woloszyn, M ; Rode, C. (2008) Modeling and Principles and Common Exercices Annex 41 Whole Building Heat, Air and Moisture Response, pp. 234, 2008 (ISBN 978-90-334-7057-8)

Zhang, Q.Y.; Huang, Y.J. (2002). Development of Typical Year Weather Files for Chimese Locations, LBNL-51436, ASHRAE Transaction, Vol. 108, part 2.